Document made available under the Patent Cooperation Treaty (PCT)

International application number: PCT/US05/008311

International filing date: 11 March 2005 (11.03.2005)

Document type: Certified copy of priority document

Document details: Country/Office: US
Number: 60/552,332
Filing date: 11 March 2004 (11.03.2004)

Date of receipt at the International Bureau: 20 April 2005 (20.04.2005)

Remark: Priority document submitted or transmitted to the International Bureau in compliance with Rule 17.1(a) or (b)

World Intellectual Property Organization (WIPO) - Geneva, Switzerland
Organisation Mondiale de la Propriété Intellectuelle (OMPI) - Genève, Suisse

1306066

THE UNITED STATES OF AMERICA

TO ALL TO WHOM THESE PRESENTS SHALL COME:

UNITED STATES DEPARTMENT OF COMMERCE

United States Patent and Trademark Office

April 07, 2005

THIS IS TO CERTIFY THAT ANNEXED HERETO IS A TRUE COPY FROM THE RECORDS OF THE UNITED STATES PATENT AND TRADEMARK OFFICE OF THOSE PAPERS OF THE BELOW IDENTIFIED PATENT APPLICATION THAT MET THE REQUIREMENTS TO BE GRANTED A FILING DATE.

APPLICATION NUMBER: *60/552,332*
FILING DATE: *March 11, 2004*
RELATED PCT APPLICATION NUMBER: *PCT/US05/08311*

Certified by

Jon W. Dudas

Under Secretary of Commerce
for Intellectual Property
and Director of the United States
Patent and Trademark Office

Substitute for PTO/SB/16 (08-03)

PROVISIONAL APPLICATION FOR PATENT COVER SHEET

This is a request for filing a PROVISIONAL APPLICATION FOR PATENT under 37 CFR 1.53(c).

Express Mail Label No. EV316084341US

INVENTOR(S)		
Given Name(first and middle[if any])	Family Name or Surname	Residence (City and either State or Foreign Country)
Weiss	Kenneth L.	Cincinnati, Ohio

☐ Additional inventors are being named on the ____ separately numbered sheets attached hereto.

TITLE OF INVENTION (500 characters max)

INTEGRATED MULTIMODALITY MULTIFUNCTIONAL SPATIAL REFERENCE AND SKIN/SURFACE MARKING SYSTEM AND AUTOMATED SPINE MRI/CT RAPID AUTOPRESCRIPTON

Direct all correspondence to: **CORRESPONDENCE ADDRESS**

☐ Customer Number 26874

OR

☒ Firm or Individual Name	**David E. Franklin, Frost Brown Todd LLC**				
Address	**2200 PNC Center**				
Address	**201 East Fifth Street**				
City	**Cincinnati**	State	**OH**	ZIP	**45202-4182**

ENCLOSED APPLICATION PARTS *(check all that apply)*

☒ Specification *Number of Pages* 28 ☐ CD(s), Number

☒ Drawing(s) *Number of Sheets* 17 ☒ Other (specify) Abstract

☐ Application Data Sheet. See 37 CFR 1.76

METHOD FOR PAYMENT OF FILING FEES FOR THIS PROVISIONAL APPLICATION FOR PATENT

☒ Applicant claims small entity status. See 37 CFR 1.27	**FILING FEE Amount ($)**
☒A check is enclosed to cover the filing fees	$80.00

☒ The Director is hereby authorized to charge filing fees or credit any overpayment to Deposit Account **06-2226**

The invention was made by an agency of the United States Government or under a contract with an agency of the United States Government

☒No

☐ Yes, the name of the U.S. Government agency and the Government contract number are:

Respectfully submitted,

SIGNATURE David E. Franklin

TYPED or PRINTED NAME **David E. Franklin**

TELEPHONE **513-651-6856**

Date March 11, 2004

REGISTRATION NO. 39,194

Docket Number 91830.0523333

USE ONLY FOR FILING A PROVISIONAL APPLICATION FOR PATENT

SEND TO: Mail Stop Provisional Application, Commissioner for Patents, P.O. Box 1450, Alexandria, VA 22313-1450.

CinLibrary/1378765.1

U.S. PROVISIONAL PATENT APPLICATION

INTEGRATED MULTIMODALITY MULTIFUNCTIONAL SPATIAL REFERENCE AND SKIN/SURFACE MARKING SYSTEM AND AUTOMATED SPINE MRI / CT RAPID AUTOPRESCRIPTION

Inventors: **Kenneth L. Weiss, MD**

Attorney Docket No.: 91830.0523333

David E. Franklin
Registration No. 39,194
FROST BROWN TODD LLC
2200 PNC Center
201 East Fifth Street
Cincinnati, Ohio 45202
(513) 651-6856 tel.
(513) 651-6981 fax
dfranklin@fbtlaw

"Express Mail" mailing label number

EV4316084341

March 11, 2004
Date of Deposit

I hereby certify that this paper or fee is being deposited with the United States Postal Service "Express Mail Post Office to Addressee" service under 37 CFR §1.10 on the date indicated above and is addressed to The Commissioner of Patents and Trademarks, Washington, D.C. 20231.

Matthew G. Burgan
(Type or print name of person mailing paper of fee)

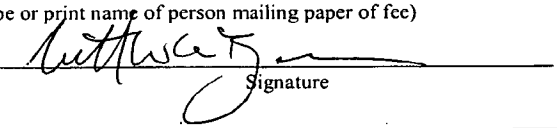

Signature

INTEGRATED MULTIMODALITY MULTIFUNCTIONAL SPATIAL REFERENCE AND SKIN/SURFACE MARKING SYSTEM AND AUTOMATED SPINE MRI / CT RAPID AUTOPRESCRIPTION

Field of the Invention

[0001] The present invention relates, in general, to medical diagnostic imaging devices that perform scout scans for localization and autoprescription.

Background of the Invention

[0002] It is often helpful to be able to obtain a one-to-one correspondence between the readily visible and markable skin/surface and underlying structures or pathology detectable by a variety of imaging modalities. This may facilitate clinical correlation, XRT, image guided biopsy or surgical exploration, multimodality or interstudy image fusion, motion correction/compensation, and 3D space tracking.

[0003] Current methods, (e.g. bath oil/vitamin E capsules for MRI), have several limitations including single image modality utility requiring completely different and sometimes incompatible devices for each modality, complicating the procedure and adding potential error in subsequent multimodality integration/fusion. They require a separate step to mark the skin/surface where the localizer is placed and when as commonly affixed to the skin by overlying tape, may artifactually indent/compress the soft tissue beneath the marker or allow the localizer to move, further adding to potential error. Sterile technique is often difficult to achieve. Furthermore, it may be impossible to discriminate point localizers from each other or directly attain surface coordinates and measurements with cross sectional imaging techniques. In regards to the latter, indirect instrument values are subject to significant error due to potential InterScan patient motion, nonorthogonal surface contours, and technique related aberrations which may not be appreciated as current multipurpose spatial reference phantoms are not designed for simultaneous patient imaging.

[0004] The trend is to take and digitally store lots of data on a patient, including MR and CT images. You want to both compare each patient's data to his/her own data, and

"pools" of data from other people. Little problem: How do you make sense of pictures taken at different times, using different types of machines and different actual machines, for the same or different people? That's what Dr. Weiss accomplishes with his techniques for the skull: well-characterized fixed reference points. He proposes something similar for the spine. Advantages: Nothing "automatic" exists today and there are no real standards for how to characterize points of reference on the skull, let alone the spine.

[0005] Consequently, a significant need exists for an improved approach to localizing and autoprescribing through multi-modal quick scans of the brain and/or spine. Furthermore, there is a need for enhancing personal medicine with a method of aligning skull and spine images.

Brief Summary of the Invention

[0006] The invention addresses the above shortcomings in a relatively simple and integrated manner. There are three major configurations of the device as follows: 1) point localizer, (2) cross-shaped grid, and (3) full planar grid/phantom. In its simplest form a multimodality visible and compatible point localizer is affixed to an adhesive fabric strip with corresponding marking so that after application and imaging the localizer can be removed with skin marking remaining. The localizer can also directly adhere to the skin. Alternatively, an ink or dye could be added to the adhesive/undersurface of the localizer to directly mark/imprint the skin obviating the fabric strip. For MRI and CT a small loop of tubing could be filled with a radioattenuative solution (e.g. containing Iodine) doped with a paramagnetic relaxant (e.g. CuS04, MgS04, Gd-DTPA). Alternatively, the tubing itself may be radiopaque for optimal CT visualization. For nuclear imaging to include planar scintigraphy, SPECT and PET, a port would be included to allow filling with the appropriate radionuclide. While the above localizers would be visible with planar radiography, a fine wire circle or dot (e.g. lead, aluminum) could be utilized with this modality given its very high spatial resolution. Other shapes and corresponding adhesive markings could be utilized to discriminate different foci and/or add further localizing capability. Additionally, an activatable chemiluminescent mixture could be added for thermography, optical

imaging, light based 3D space tracking or simply improved visualization in a darkened environment.

[0007] In the second major configuration, a unique cross shaped grouping of prefilled or fillable tubing is utilized as a grid for cross sectional imaging with the number and position of tubes imaged in the axial or sagittal planes corresponding respectively to the slices z or y distance from the center. For planar radiography, a flexible radiopaque ruled cross shaped grid is employed. Both grids are removable from similarly ruled cross shaped adhesive strips after patient application and imaging.

[0008] Lastly, a unique essentially planar grid/phantom is described which may be of flexible construction and reversibly affixed to an adhesive/plastic sheet with corresponding grid pattern for skin marking and to serve as a sterile interface between patient and reusable grid/phantom. The grid/phantom may also be directly adherent to the skin for guided aspiration or biopsy with the cross sectionally resolvable spatial reference in place. A diagonally oriented prefilled or fillable tube overlies a grid like lattice of regularly spaced tubing so that slice location and thickness can be readily determined in the axial and sagittal planes. Additionally, the spatial accuracy of the imaging modality could be assessed and, if individual tubes are filled with different solutions, multipurpose references for MR/CT, and nuclear imaging could be achieved. Furthermore, if the tubing is surrounded by a perflurocarbon or other uniform substance without magnetic susceptibility, MR imaging could be improved by reducing skin/air susceptibility and motion artifact. Additionally, the grid/phantom could be incorporated in routinely utilized pads and binding devices with or without skin adhesion and marking.

[0009] These and other objects and advantages of the present invention shall be made apparent from the accompanying drawings and the description thereof.

Brief Description of the Fig.ures

[0010] The accompanying drawings, which are incorporated in and constitute a part of this specification, illustrate embodiments of the invention, and, together with the general description of the invention given above, and the detailed description of the embodiments given below, serve to explain the principles of the present invention.

[0011] Fig. 1 illustrates the point localizer. Fig. 1a is a frontal view of the localizer affixed to the fabric. FIG. 1b depicts the reverse side. Fig. 1c is a perspective view of the localizer and underlying fabric affixed to the skin. Fig. 1d is an enface view of the fabric with corresponding marking affixed to the skin. Fig. 1e is an enface view of the localizer affixed to skin. It demonstrates a port integrated into the tubular ring. Fig. 1g is a frontal view of a modified ring shaped localizer affixed to- fabric with additional markings. Fig. 1h is a frontal view of the fabric in Fig. 1g with the localizer removed. Fig. 1i is a frontal view of a multilocalizer sheet demonstrating the adhesive backing and overlying fabric with localizers removed.

[0012] Fig. 2 illustrates the cross-shaped grid configuration 2a is an enface view of the grid with modified square as the central hub and uniquely positioned rows of tubing radiating along the vertical and horizontal axes. Fig. 2b is a schematic of axial cross sections acquired at representative distances from the horizontal axis. Fig. 2c demonstrates the underlying marked fabric with the superimposed tubing in 2a removed. Fig. 2d is a variant of Fig. 2a with modified ring serving as a central hub. Fig. 2e depicts a limb fixation ring and angulation adjuster. Fig. 2f depicts a radiopaque grid with underlying ruled fabric strips removed.

[0013] Fig. 3a is an enface view of the grid/phantom configuration with tubular lattice, overlying a diagonally oriented slice indicator, and underlying a partially adhesive fabric with markings and perforations. Fig. 3b is a schematic cross section of a representative axial section.

[0014] Fig. 4 is localizers in a packaged strip or roll, regularly spaced at 5 cm or other intervals.

[0015] FIG. 5 is a lattice localizer having tube diameters varied to identify unique locations.

[0016] FIG. 6 is a full-spin grid localizer and spinal coil.

[0017] FIG. 7 is a midline roll- and yaw-corrected sagittal fast spin-echo T2-weighted MR image (TR/TE, 3816/105_{eff};echo train length, 16; section thickness, 4 mm; matrix 512 x 256; field of view, 20 cm). The short solid line corresponds to the Talairach AC-PC basal reference; the long solid line is drawn parallel to the Talairach AC-PC

reference, and the dashed line passes through the superior cortical surface of the hard palate. Note in this prototypical case the angle subtended by the Talairach AC-PC line and the hard palate is 12°. AC, anterior commissure; PC, posterior commissure; HP, hard palate.

[0018] FIG. 8 is a lateral CT scout view from a study patient illustrating the axial scan prescription *(dotted lines)* with the HP+ 12 protocol angled +12° from a line passing through the hard palate *(solid line)*. The solid line indicating the orientation of the hard palate has been offset a few millimeters inferiorly to provide a clear view of the hard palate.

[0019] FIG. 9 is consecutive CT and MR examinations from the same subject taken on different days by using the HP+12 CT protocol and a direct Talairach referenced MR imaging protocol (3). First row illustrates axial CT and MR image prescription methodologies. Note in this archetypal patient the angle subtended by the hard palate and the AC-PC line as depicted on the sagittal T2-weighted MR image is 12°, matching the CT prescription protocol. The second and third rows illustrate a representative axial section from these examinations through the orbits and posterior fossa with differing CT windows or MR sequencing. Axial CT and MR sections are 5 mm and 4 mm thick, respectively. Note the excellent intra- and intermodality axial scan concordance.

[0020] Fig. 10 is a sequential illustration of the three-step clinical protocol.

[0021] Fig.. 11 is an illustration of key algorithms for identifying the anterior and posterior commissures.

[0022] Fig.s. 12A-C include a (a) search window and its intensity projection. (b) extracted inter-vertebral disc contour, and (c) contour extraction of an MRI spine.

[0023] FIG.. 13A-B are sagittal images illustrating the contiguous 35cm FOV two-station technique (FGRE TR 58, flip 30 degrees, TE 2.0, 512x352 matrix, 21 sec each). The woman on left has a straight spine, while woman on right has mild scoliosis.

Detailed Description of the Invention

[0024] **Integrated multimodality, multi-functional spatial reference and skin/surface marking system.**

[0025] Fig. 1 illustrates the preferred embodiments of the point localizer. In 1a, a loop of prefilled tubing (10) is shown superimposed on and reversibly affixed to an underlying medical grade fabric (11), which may double as an adhesive bandage to both cover and mark a wound or puncture site. The tubular ring's diameter may be 2 cm mid luminal, as illustrated, or outer luminal, as perhaps preferable for integration with the cross shaped grid configuration. Other sized rings, to include in particular a 1 cm. diameter, may also have merit. The tubal lumen should measure 2-5 mm in diameter. Cross sectional images through the ring will have characteristic and quantifiable appearances depending on slice thickness and distance from the center. A thin slice through the loop's center, for example, would demonstrate 2 circles of luminal diameter whose centers are separated by a distance equal to the ring's diameter.

[0026] The tube lumen can be filled with an appropriate concentration of an iodinated contrast agent for optimal CT visualization doped with a paramagnetic relaxant such as CuS04,MgS04, or GdDTPA to maximize MRI signal via preferential T1 shortening. Alternatively, the tubing itself may be optimally radiopaque for CT, obviating the iodinated contrast. If desired, for optical imaging, thermography, light based 3D space tracking, or improved visibility in a darkened environment, one could add an activatable chemiluminescent mixture whose critical reagents are separated by a membrane readily breached by external force applied to the ring.

[0027] A slightly redundant backing (12) is provided for the adhesive side of the fabric to facilitate peeling (Fig. 1b arrows) and skin placement. With backing removed, the unit adheres to the skin (13) as depicted in Fig. 1c. After imaging, the loop which has its own adhesive undersurface, may be removed revealing the underlying fabric marking (14) as in Fig. 1d. The upper surface of the fabric, or circumscribed area thereof, would also have adhesive backing-like properties to facilitate detachment of the ring. Once separated from the fabric, the loop could also directly adhere to the skin as in Fig. 1e. Additionally, the adhesive undersurface of the ring could contain a medical grade dye or

ink so that a corresponding imprint would be left on the skin after removal, potentially obviating the fabric marker.

[0028] A port (15) may be directly integrated into the tubular ring as in Fig. 1f, and a vacuum created within the lumen to facilitate filling at the imaging center. This feature would be critical for radionuclide scans and add flexibility for other imaging studies.

[0029] To increase spatial reference capability and allow multiple localizers to be discriminated from each other, the ring and underlying fabric marking may be modified as in Figs. 1g and 1h. As illustrated, two tubular spokes (16) at right angles to each other may be added with luminal diameter less than or equal to that of the loop. Typically, the modified ring would be positioned on the patient so that the spokes are aligned at 0 and 90 degrees as perhaps determined by the scanner's alignment light. Subsequent rings could be progressively rotated 90 degrees so that quadrants I, II, III, and IV are sequentially subserved by the spokes. With the simple ring included, this would provide 5 distinguishable localizers. Moreover, if stacking of two rings is utilized, 30 (5x6) distinguishable localizer configurations are possible. Suggested numbering would employ .the base 5 system, assigning the simple ring the value 0 and each modified ring the value of the quadrant subserved.

[0030] Multiple localizers may also be dispensed on a single sheet rather than individually packaged. Fig. 1i illustrates such a sheet, demonstrating the adhesive backing (17) and overlying fabric (11) with the simple ring (left side) and modified ring (right side) localizers removed. Tabs (18) have been added to the fabric to facilitate both removal of the unit from the backing and the localizer from the fabric. Discontinuity of the backing (solid lines (19)) underlying the tabs would also simplify removal of the fabric from-the backing and perforations through the backing (dotted lines (20)) would facilitate separation of individual units from each other. If desired, a smaller diameter (e.g. 1cm) ring and associated backing albeit without tab could be placed within the central space (21) bordered by the simple ring fabric (19).

[0031] Embodiments of the prefilled or fillable cross shaped grid configuration are illustrated in Fig. 2. In Fig. 2a, a modified tubular square (21) with diagonal dimensions of 2 cm and containing 2 smaller caliber spokes at right angles to each other (23) serves as the hub. Uniquely positioned rows of tubing (24) radiate from each corner along the

vertical and horizontal axes. The luminal diameter of the radiating tubes is uniform and on the order of 2 mm. except where indicated by dotted lines (25) corresponding to gradual tapering from 0 to the uniform diameter. Depending on the distance from the central hub, 1 or 2 rows of tubing will be present with up to 4 tubes in each row as best illustrated in Fig. 2b. The lower row of tubes (i.e. closest to skin) would correspond to increments of 1 cm. and the upper row to increments of 5 cm so that a maximum distance of 24 cm would be denoted by 2 full rows. To indicate positive distances, the tubes are progressively ordered from left to right or down to up with the reverse true for negative distances as illustrated in Figs. 2a,b. Fractions of a centimeter would be indicated by the diameter of a cross section through a tapered portion of tubing divided by the full uniform diameter.

[0032] The cross-shaped grid of tubing is reversibly affixed to a medical grade adhesive fabric with corresponding markings and backing. The fabric (26) is illustrated in Fig. 2c with the overlying tubing removed. The grid and associated fabric may come as a single cross-shaped unit or as a modified square and separate limbs which could be applied to the patient individually or in various combinations. Modified squares could also link whole units and/or individual limbs together to expand coverage, with 25 cm. spacing between the center of adjacent squares. The tubing may be flexible to allow the limbs to conform to curved body contours such as the breast. Additionally, either the limbs could be readily truncated at 5 cm. intervals or be available in various lengths for optimal anatomic coverage.

[0033] To add further utility and integration with the previously described point localizers, a modified ring may serve as the hub of the cross-shaped grid with associated modification of the limbs as illustrated in Fig. 2d. The orthogonal limbs would not have to maintain a coincident relationship to the spokes as with the modified square hub. Rather, by first placing and rotating a calibrated ring adapter (Fig. 2e) about the modified loop, 1 to 4 limbs could be readily positioned at any desired angle relative to the spokes. Pairs of male plugs (27) extending from the ring, adapter would fit securely into corresponding holes (28) at each limb base to ensure proper positioning. It is foreseen that one would typically align the modified ring's spokes with the scanner's axes and the ring adapter/limbs with the axes of the body part to be studied. By noting the chosen

angulation marked on the ring adapter, optimal scanning planes might be determined prior to imaging.

[0034] For planar radiography, a cross-shaped grid of radiopaque (e.g. lead or aluminum) dots at 1 cm intervals interposed by 5 cm spaced dashes (Fig. 2e) would minimize the imaging area obscured by overlying radiopacity. The minute opacities could be reversibly affixed by clear tape to an underlying marked adhesive fabric similar to that illustrated in Fig. 2c. Alternatively, similarly spaced radiopaque dots and dashes could be dispensed reversibly affixed to a role of medical grade adhesive tape with corresponding markings. Any length of this dually marked taped could be applied to the patient to include a single dot as a point localizer.

[0035] In the planar grid/phantom configuration, 1 cm spaced horizontal and vertical tubes form a graph paper-like lattice as illustrated in Fig. 3a. Tubes at 5 cm intervals (29) would have larger luminal diameters (e.g. 3mm) than the others (e.g. 2mm). The central vertical (30) and horizontal (31) tubes would have a smaller diameter (e.g. 1 mm). Overlying the lattice at a 45 degree angle is the slice indicator tube (32). Depending on the distance from the horizontal or vertical axes respectively, axial or sagittal cross sections through the grid/phantom (GP) would demonstrate the slice indicator uniquely positioned as it overlies a row of 1 cm spaced tubes. Fig. 3b illustrates a representative axial slice obtained 6 1/2 cm above the horizontal axis. Note that the cross section o£ the slice indicator is positioned above and midway between the sixth and seventh tubes to the right o£ the sectioned vertical axis (30). Additionally, the thickness (t) of the image section can be readily determined as it equals the cross-sectional width (w) of the indicator minus the square root of 2 times the diameter (d) of the indicator lumen,(t = w - V2" d).

[0036] The GP may be reversibly affixed to an adhesive/plastic sheet with a corresponding graph paper-like grid for skin marking and to serve as a sterile interface between the patient and GP. Perforations (33) may be placed in the sheet as shown in Fig. 3a to allow ready separation of a cross-like ruled adhesive fabric (similar to that illustrated in Fig. 2c), from the remaining plastic sheet after imaging and removal of the GP.

[0037] The square GP should have outer dimensions equal to a multiple of 10 cm (e.g. 30 cm as illustrated) to allow for simple computation if GPs are placed side to side for expanded surface coverage. Adapters could be provided to ensure secure and precise positioned of adjacent GPs either in plane or at right angles to each other. The GPs can be flexible or rigid in construction and be utilized with or without skin adhesion and marking.

[0038] Tubes may be filled uniformly or with a variety of known solutions having different imaging properties to serve as multipurpose references. For the latter, the 5 cm spaced tubes and slice indicator may be filled with the same optimized solution as previously described, while each set of 4 intervening tubes could be filled with different solutions in similar sequence. In this fashion, identical series of 5 reference solutions would repeat every 5 cm, allowing intraslice signal homogeneity to be assessed as well. If 9 rather than 5 different solutions are desired, sequences could instead be repeated every 10 cm. For MRI, the central tubes may also be surrounded by an oil/lipid within a larger lumen tube to serve as both a lipid signal reference and allow for measurement of the fat/water spatial chemical shift. Furthermore, if the GP tubing is surrounded by a perflurocarbon or other substance without magnetic susceptibility, MR imaging could be improved by reducing skin/air susceptibility artifact and dampening motion. The GP may also be incorporated into a variety of nonmodality specific pads (including the ubiquitous scanner table pad(s)), binders, compression plates, biopsy grids and assorted stereotaxic devices.

[0039] Two additional variations are now described, potentially replacing the somewhat complex cross design (Fig. 2) with an extension of the basic point localizer (Fig. 1) or modification of the planar phantom/localizer (Fig. 3). These changes may further simplify and unify the proposed marking system.

[0040] In the first instance, rather than packaging the ring localizers in a sheet as illustrated in Fig. 1i, they could be packaged in a strip or roll, regularly spaced at 5 cm or other intervals (Fig. 4a). The strip with attached ring and/or cross localizers could then serve as a linear reference of any desired length. By placing two strips orthogonally, a cross-shaped grid is created. Individual rings can be removed from the strip or rotated to customize the grid as desired (Fig. 4b).

[0041] In the second instance, by slightly modifying the square design illustrated in Fig. 3, an elongated rectilinear or cross configuration (Fig. 4a) is achieved consisting of linearly arranged squares extending vertically and/or horizontally from the central square. One tube in each of these squares will have a larger diameter than the other similarly oriented tubes as determined by the square's distance from the isocenter. For example, the square centered 10cm above the isocenter would have its first tube situated to the right of midline given an increased diameter and the square centered 20 cm above the isocenter would have its second tube to the right of midline given an increased diameter and so on.

[0042] Cross sectional distance from isocenter would be read by adding the distance determined by each square's diagonally oriented slice indicator to 10 times the numberline position of the largest diameter tube. Figure 5b illustrates the cross sectional appearance of an axial section obtained 12 1/2 cm. above isocenter. By adding 2 1/2 (the slice indicator position) to 10 times 1 (the tube with largest diameter), distance is readily determined.

[0043] Alternatively, the caliber of all tubes could be kept constant and instead an additional diagonal indicator tube passing through isocenter added for each elongated axis (vertical with slope of 10 and horizontal with slope of 1/10). Cross-sectional distance from isocenter would then be determined by looking at the position of both the additional and original diagonal indicator tubes in reference to the cross sectionally-created number line.

[0044] It should also be noted that localizer grids similar to those illustrated in Figs. 3 and 5 could be constructed of barium (or other high x-ray attenuative material) impregnated sheets rather than tubes if computed tomography is the primary imaging modality desired and phantom attenuation values are not needed. This would significantly reduce the cost of the grid, allowing disposability and retaining 1:1 compatibility with the multifunctional tube filled grid/phantom.

[0045] **Flexible phased array surface coil with integrated multimodality, multifunctional spatial reference and skin/surface marking system.**

[0046] The invention may be modified to include a sheath for and inclusion of a flexible array MRI surface coil. Positioned vertically, this device could be closely applied to the entire cervical, thoracic, and lumbar-sacral spine. Additionally, the quantity of tubes which need to be filled in the planar configuration to uniquely denote cross-sectional positioning, has been substantially reduced from the original embodiment.

[0047] Phased array surface coils significantly increase signal to noise in MRI and are commonly employed for spine imaging. Currently, such spine coils are rigid and planar in configuration. As such, patients can only be effectively scanned in the supine position, lying with the back against the coil. This results in signal drop-off in regions where the spine/back is not in close proximity to the planar coil, particularly the lumbar and cervical lordotic regions. The invention, described herein, would reduce the signal drop-off and allow patients to be scanned in any position. The prone position, for example, would facilitate interventional spine procedures that could not be performed with the patient supine. Patients could also be more readily scanned in flexion or extension; or with traction or compression devices. Current surface coils also lack an integrated spatial reference and skin marking system. Inclusion of the proposed spatial reference and skin marking system would facilitate multi-modality image fusion and registration as well as the performance of diagnostic or therapeutic spine procedures, such as biopsies, vertebroplasty, or XRT.

[0048] As illustrated in Fig. 6a, a grid-localizer would be adhered to the patient's spine. Tubing would be filled with a MRI readily-visible solution such as water doped with CuSO4. The grid itself would typically be 10 cm wide and 70-90 cm in length to cover the entire spine. An attached clear plastic sheath would allow introduction of a flexible array coil such as illustrated in Fig. 6b.

[0049] The configuration of tubing would allow unambiguous determination of the MRI scan plane (axial or sagittal) in reference to the patient's back/skin surface. The number of thin caliber tubes could denote the distance from (0,0) in multiple of 10cm as illustrated in Fig. 6b (those to the right or superior would be positive; those appearing to the left or inferior would denote negative distances). Alternatively, as illustrated in Figs. 6c,d, the integer distance in centimeters from a single thin tube to the central tube could be multiplied by ten to denote distance from (0,0). Thus, 30 cm could be denoted by a

single thin tube 3cm from the central tube rather than by 3 thin tubes as in Fig. 6b. As illustrated in Figs. 6c,d, an axial slice taken 8cm superior to (0,0), would reveal the cross sectional tubes illustrated in 6d. The thin tube being 1cm to the right of the central tube would denote a vertical distance of 10cm. The diagonal oriented tube in cross-section, being 2 cm to the left of the central tube, would denote a vertical distance of -2cm. Thus, the axial plane of section would be 10-2=8cm above (0,0).

[0050] Using the described reference/marking system affixed to the patient's back, a diagnostic or therapeutic procedure could be performed under direct MR guidance. Alternatively with a corresponding radiopaque grid affixed to patient's back, the patient could be taken out of MRI scanner and have the procedure done with CT or fluoroscopic guidance. In either case, procedures could be performed by hand or with a robotic arm.

[0051] **CT Brain Prescriptions in Talairach Space: A New Clinical Standard.**

[0052] *BACKGROUND AND PURPOSE:* Head CT prescriptions are currently plagued by intra- and intersubject image variance and do not match standardized MR imaging planes. We developed and tested a simple method to improve CT precision and approximate the Talairach reference standard advocated for MR imaging.

[0053] *METHODS:* We retrospectively reviewed midline sagittal T2-weighted brain MR images of 126 consecutive patients to determine the mean angle subtended by the Talairach anterior commissure-posterior commissure (AC-PC) line and the hard palate. On the basis of this data set, a new head CT protocol was instituted with pitch similarly prescribed relative to the hard palate as identified on the lateral CT scout film. We then compared the precision of the new protocol, our former method (nominally parallel to the orbito-meatal line) and fixed-gantry angulation. Two head CT studies from 50 consecutive patients imaged with our old protocol and 50 consecutive patients imaged with our new protocol were reviewed for a total of 200 CT examinations.

[0054] *RESULTS:* The Talairach AC-PC line was rotated 12.0° t 6.1° from the hard palate line and 15.6° -*F* 10.1° from the axial plane of the magnet. The new CT protocol approximated the Talairach-referenced MR images obtained at our institution and improved intrapatient CT scan precision compared with fixed-gantry selection (P <

.004) and compared with our previous prescription technique ($P < .064$; $P < .025$, controlling for excessive head extension).

[0055] *CONCLUSION:* By prescribing CT images angled +12° from the hard palate, a structure readily identified by technologists, interscan precision can be improved and Talairach-referenced MR imaging studies can be approximated. Along with AC-PC-referenced MR imaging studies, we advocate this CT protocol as a new clinical standard.

[0056] Variability in head positioning and prescribed techniques for MR imaging and CT may yield significant intra- and intersubject image variance within and across modalities. Having already become a *de facto* standard for neuroscience research and stereotaxis, the Talairach reference has been recently advocated as a new standard for clinical brain MR imaging (1-4). Recently, both technologist- and computerdriven methods to directly prescribe Talairach-referenced MR images have demonstrated a substantial reduction in interpatient scan variance and more efficient brain coverage than routine clinical axial imaging (3).

[0057] CT head scans have been traditionally prescribed parallel to the orbito-meatal line (OML), defined as passing through the lateral canthus and middle of the external ear canal (5-7). Use of this external reference line for CT prescriptions, however, has several major drawbacks. First, it is difficult to discern the OML on the lateral scout view from which technologists currently prescribe. Second, if a patient's head is extended, scanner limitations in gantry angulation (e.g., 22° for most GE CT scanners [General Electric Corporation, Milwaukee, WI]) may preclude accurate OML prescription. These two factors can lead to significant prescription errors and inter- and intrasubject CT image variance. In addition, the OML may have a relatively inconstant relationship to superficial and deep brain structures, resulting in further inter-subject variance in the appearance of the brain on axial CT sections (8). Finally, the OML matches neither conventional MR axial sectioning nor Talairach anterior commissure-posterior commissure (AC-PC)-referenced imaging, being approximately 24° steeper than the former and 9° steeper than the latter (3). As a result, axial head CT scans parallel to the OML may be difficult to directly

compare with axial brain MR imaging sections, particularly those conventionally prescribed orthogonal to the bore of the magnet.

[0058] We developed and tested a simple method to improve CT precision and approximate the Talairach reference standard advocated for MR imaging by using the hard palate as a landmark. The hard palate was selected because it is a relatively planar midline structure fixed to the skull and projects as a line on the lateral CT scout film. In addition, this readily identifiable landmark is already used by technologists to prescribe maxillofacial CTs.

[0059] *Methods*. Institutional review board approval was obtained. Subsequently, to determine the mean angle subtended by the Talairach AC-PC line and the hard palate, two co-authors (KL. W. and J.S.) retrospectively reviewed a data base of 126 midsagittal, T2-weighted clinical brain MR images produced from May 7, 2002 to May 21, 2002 at our institution. (Fig. 7) The MR imaging population consisted of 64 male and 62 female subjects ranging in age from 17 to 89 years, with an average age (±SD) of 49.2 (±17.8) (3). On November 15, 2002, we instituted a new clinical head CT protocol (HP +12) in which scan pitch (gantry tilt) was to be offset by this predetermined angle relative to the hard palate as identified by technologists on the lateral CT scout film (Fig. 8). This protocol replaced our former protocol (OML*) in which the technologists were instructed to angle the gantry parallel to the OML as visualized on the lateral scout, albeit difficult to identify. The asterisk designates the technologist approximation of the OML from the lateral scout rather than the true anatomic OML.

[0060] To compare the performance of our new protocol (HP +12) against our former protocol (OML*) and an alternate hypothetical fixed-gantry protocol (AX+15) optimized to approximate the Talairach AC-PC line, we reviewed a total of 200 head CT examinations. These included 50 consecutive patients with two head CT studies taken by using the OML* protocol and 50 consecutive patients with two head CT studies taken with the HP+ 12 protocol. The CT scan population consisted of 56 male and 44 female subjects. Patient age was only available for 57 of the patients and ranged from 16 to 93 years, with a mean of 49.8 years (± 17.6).

[0061] For each CT study, the lateral CT scout and technologist selected gantry angle for axial sections were collected for review, the latter obtained from the DICOM header. Hard palate angles relative to the horizontal plane were measured independently on all

200 CT scouts by three co-authors (K.L.W., J.L.W., and W.S.) and were subsequently reviewed together by the same three co-authors *en banc* to establish a hard-palate angle consensus and determine a gantry detector tilt co-author-derived criterion standard. For the alternate fixed-gantry protocol, the average hard palate angle was used. The sign convention for angle measurements defines head extension as positive.

[0062] Pearson correlation coefficients were compared for the OML* and HP +12 protocols. Precision and accuracy relative to the co-author criterion standard for each gantry tilt method was also evaluated. The accuracy of a particular study was measured as the absolute difference between the technologists elected gantry angle and the co-author criterion standard:

1) $E_{\text{accuracy}} = | \theta_{\text{CT gantry}} - \theta_{\text{CT standard}} |$

The precision or reproducibility of each method was calculated as the absolute difference in prescription accuracy for each pair of CT scouts obtained from the same subject:

2) $E_{\text{precision}} = | (\theta_{\text{CT1 gantry}} - \theta_{\text{CT1 standard}}) - (\theta_{\text{CT2 gantry}} - \theta_{\text{CT2 standard}}) |$

[0063] To adjust for population bias and isolate the influence of our CT scanner's 22° maximum gantry tilt limitation, full and reduced data sets for the OML* and HP+ 12 technologist method protocols were compared. The reduced data set consisted of only those scans requiring a gantry tilt less than or equal to 22° as determined by the co-author-derived hard-palate criterion standard.

[0064] Statistical analysis was performed by using DSTPLAN, NCSS 2001, and Microsoft Excel (9-11). A statistical significance threshold of a = 0.05 was applied for all inferences.

[0065] *Results.* Paired measurements of the Talairach AC-PC reference and hard palate could be obtained for only 117 of the 126 MR imaging studies because of distorted anatomy, artifact, or limited field of view. For these 117 studies, the Talairach AC-PC line was extended by 12.0° (±6.1°) from the hard palate line and 15.6° (±10.1°) from the axial plane of the magnet. Consequently, to approximate the Talairach AC-PC line protocol the HP +12 CT protocol prescribes CT gantry detector tilt at +12° extension from the hard palate as identified by the technologists on lateral CT scout film.

[0066] Average technician-prescribed gantry tilt by using the OML* protocol was 11.1° (±8.6°) and 13.4° (± 7.5°) by using the HP+12 protocol. In all 200 CT lateral scout images, a co-author consensus for the hard palate orientation was achieved. Interauthor correlation coefficients for hard palate angle measurements from the CT lateral scout ranged from 0.90 to 0.95, and individual author correlation with the hard palate criterion standard ranged from 0.94 to 0.98. The hard palate in all lateral scout CTs studied was extended an average 3.0° (± 11.9°).

[0067] Overall, the standard hard palate extension averaged 3.0° (±11.9°). For the alternate hypothetical fixed-gantry protocol (AX +15) we chose a fixed-gantry tilt of 15° to best approximate the Talairach AC-PC line as extended +12° from the overall average hard palate angulation of 3.0° on lateral scout CT to arrive at a hypothetical fixed-gantry tilt of 15°.

[0068] The patient heads studied with the HP + 12 protocol were more extended than those studied with the OML* protocol. This introduced a significant population bias, in view of the 22° maximum gantry tilt permitted on our GE scanners. To compensate for this bias, a reduced data set was created by selecting only CT scans that require gantry prescriptions no greater than 22°. The reduced data set excludes 56 (25 OML* scans and 31 HP + 12 scans) of the 200.

[0069] The difference in correlation of the OML* (R = 0.78) and HP+12 (R = 0.82) prescriptions with the co-author criterion standard was not statistically significant when comparing full data sets (P = .18; power = 0.23; Table 1A). The HP+12 method, however, was more strongly correlated with the criterion standard (R = 0.87) than was the OML* method (R = 0.69) for the reduced data set (P < .003; power = 0.87; Table 1B) Correlation analysis does not apply to the AX+15 fixed-gantry protocol because a constant prescription of 15° was used.

[0070] Due to the use of absolute values, the distributions of accuracy and precision metrics were significantly nongaussian. To derive inferential statistics, data transformations were tested (12). Cubic-root transformation was found to significantly improve the normalcy of all variables and was subsequently applied.

[0071] Both the HP +12 and OML* technologist protocols were more accurate than the fixed-gantry AX+15 alternative ($P < .0001$). There was no statistical difference between the accuracies of the HP+12 and OML* protocols for the full data set ($P = .71$; power = 0.07; Table 1A) For the reduced data set, however, the accuracy of the HP+12 protocol was superior to that of the OML* protocol ($P = .004$; power = 0.83; Table 1B).

[0072] The HP+12 protocol was more precise than the fixed-gantry alternative AX+15 protocol ($P = .004$; power = 0.85). The OML* protocol did not significantly improve precision relative to the fixed-gantry AX+15 protocol ($P = .18$; power = 0.24). There was also evidence of improved precision by using the HP + 12 protocol relative to the OML* protocol, but this did not demonstrate statistical significance at $a = 0.05$ for the full data set ($P = .06$; power = 0.46; Table 1A). For the reduced data set, the precision of the HP+12 protocol was superior to that of the OML* protocol ($P = .025$; power = 0.63; Table 1B).

[0073] *Discussion.* Institution of the aforementioned CT prescription protocol was easy for our technologists and did not require special training. Concurrently, we changed our routine section thickness from 5 mm through the posterior fossa and 10mm above to contiguous 5-mm-thick sections through the entire brain. This simplifies brain prescriptions, improves interscan image concordance by reducing maximum offset from 5 to 2.5mm, permits subsequent whole brain multiplanar reconstructions on our multidetector scanners, and better approximates our routine 4-mm MR imaging brain sectioning. In addition, we reduced our field of view from 25 to 22cm to increase in-plane spatial resolution and better approximate our MR imaging studies typically performed with a 20-cm field of view.

[0074] Although readily identifiable on lateral CT scout films, the hard palate may have some limitations as a landmark for pitch determination. The superior surface of the hard palate appears grossly planar, but curvature may exist (13). Coupled with the relatively short anteroposterior dimension of the hard palate, this curvature could yield some inherent interobserver error. Nonetheless, as hypothesized, using the hard palate as a landmark did improve CT scan precision and accuracy relative to fixed-gantry angulation and to the OML* and AX+15 protocols, the latter nominally

relying on the OML. Unexpectedly, the technologist-selected OML* was less extended than the HP+12 line designed to approximate the Talairach AC-PC reference. Two factors could be contributory, either our technologists were choosing landmarks offset from the patient's actual OML or the patient population did not approximate the 305 healthy volunteer Montreal Neurological Institute brain population in this measurement (3). In light of the difficulty of discerning the OML on lateral CT scout films, we believe the former factor likely predominates, hence the asterisk in the OML* designation.

[0075] By approximating the Talairach AC-PC line in an individual patient, the HP+12° protocol may be discordant with the Talairach reference, reducing CT-MR imaging intermodality precision. In our study, the angle subtended by the hard palate and the AC-PC line varied from patient to patient (SD = 6.3°). Consequently, excellent CT-MR imaging concordance as demonstrated in Figure 9 would be expected to occur only when an individual's subtended angle closely approximates the mean of 12°. (Fig.s 7 and 9)

[0076] To improve intermodality image concordance, implementing the HP+12° CT algorithm should ideally be done in conjunction with adoption of the Talairach MR imaging reference standard. If for technical, anatomic, or pathologic reasons technologists can identify the hard palate but not the AC and PC on a patient's midline sagittal MR imaging, the MR imaging study could be prescribed in a similar fashion to that suggested for brain CT scans; that is, 12° steeper than the hard palate. Theoretically, this should further reduce CT-MR imaging intermodality variance while approximating the desired Talairach AC-PC pitch.

[0077] In contradistinction to the three-step protocol proposed by Weiss and co-authors for providing direct Talairach-referenced MR imaging examinations, the CT protocol does not compensate for patient roll and yaw (2, 3). Consequently, to optimize CT results, care should be given to ensure that the patient's head is not significantly rotated within the head holder/gantry. Moreover, when using a CT scanner constrained by a maximum gantry tilt of less than 30°, significant head extension should be avoided as much as possible. Unfortunately, in the acute trauma setting, technologists may not be able to readily or safely reposition the patient's head.

[0078] In view of the study's urban trauma level-one medical center setting and the two-CT-examination inclusion criteria, our scan population was strongly biased to acute traumatic injury. Consequently, higher precision might be expected in a different setting, such as an outpatient imaging facility or with CT scanners that permit greater gantry angles. Because our study did not include infants or children, the results may not yet be generalized outside the adult population. Further investigation is currently under way to include evaluation of the proposed methodology in pediatric patients.

[0079] *Conclusion.* By prescribing CT images angled 12° from the hard palate, interscan precision can be improved and Tailarach-referenced MR imaging studies can be approximated. Along with Talairach AC-PC-referenced MR imaging studies, we advocate this CT protocol as a new clinical standard. Adoption of these complementary CT and MR imaging prescription protocols should facilitate intra- and intermodality comparisons, leading to more reproducible and readily interpretable brain imaging findings.

[0080] *References:*

1. Talairach J, Tournoux P. *Co-planar Stereotaxic Atlas of the Human Brain.* New York: Thieme; 1988;

2. Weiss KL, Dong Q, Weadock WJ, et al. Multiparametric colorencoded brain MR imaging in Talairach space. *Radiographics* 2002; 22:E3-E3;

3. Weiss KL, Pan H, Storrs J, et al. Clinical brain MR Imaging prescriptions in Talairach space: technologist- and computerdriven methods. *AJNR Am J Neuroradiol* 2003;24:922-929;

4. Nowinski W. Modified Talairach landmarks. *Act Neurochirurgica* 2001;1045-1057;

5. Talairach J, Tournoux P. Cerebral structures in three-dimensional space. In: Talairach J, Tournoux P, eds. *Co-planar stereotaxic atlas of the human brain.* New York: Thieme; 1988:19;

6. Fleckenstein P, Tranum-Jensen J. Principles and techniques. In: *Anatomy in Diagnostic Imaging.* 2nd ed. Philadelphia: WB Saunders; 2001:50;

7. Runge V, Osborne M, Wood M, et al. The efficacy of tilted axial MRf of the CNS. *Magn Reson Imaging* 1987;5:421-430;

8. Gao F, Black S, Leibovitch F, et al. A reliable MR measurement of medial temporal lobe width from the Sunnybrook Dementia Study. *Neurobiol Aging* 2003;24:49-56;

9. Hintze *J. NCSS and PASS.* 2001 ed. Kaysville, Utah: Number Cruncher Statistical Systems, 2001;

10. Brown BW, Brauner C, Chan A, et al. *DSTPLAN.* 4.2 ed. Houston: University of Texas MD Anderson Cancer Center Department of Biomathematics, 2000;

11. Microsoft. *Microsoft Excel.* 2002 SP-2 ed. Redmond, WA: Microsoft, 2001;

12. Murphy E. Transformations. In: Murphy E, ed. *Biostatistics in medicine.* Baltimore: Johns Hopkins University Press; 1982:70-72 13. Gray H. Splanchnology. In: Williams P, Warwick R, Dyson M, Bannister L, eds. *Gray's anatomy.* New York: Churchill Livingstone; 1989:1289.

		Accuracy			Precision		
Protocol	R	Mean	SD	N	Mean	SD	N
A. Full Data Set[a]							
AX + 15		9.36°	7.38°	200	7.53°	5.11°	100
OML*	0.78	5.73° [c]	4.56°	100	6.67°	5.34°	50
HP + 12	0.82	5.98° [c]	5.73°	100	5.32° [c]	4.38°	50
B. Reduced Data [d]							
AX + 15		7.18°	6.78°	147	7.34°	5.38°	66
OML*	0.69	4.87° [c]	3.99°	78	6.77°	5.97°	35
HP + 12	0.87 [d]	3.27° [c, d]	2.87°	69	4.37° [c, d]	3.79°	31

Table 1: Comparative performance of prescription protocols

[a] Results for the full data set.

[b] Results controlled for head extension requiring gantry tilt prescription greater than 22°.

[c] Significant improvement ($P < 0.05$) versus AX + 15 protocol.

[d] Significant improvement ($P < 0.05$) versus OML* protocol.

[0081] Iterative Scan Presciptions for Optimized Magnetic Resonance Imaging (MRI) of the Neuro-Axis. The investigators from UC have recently developed offline algorithms

and an associated three-step clinical protocol, as shown in Fig.. 10 that can rapidly, accurately, and reproducibly prescribe the imaging planes of brain MRIs (Weiss et al. 2003). A series of scout images allows the anterior and posterior commissure landmarks that form the basis of the Talairach reference to be identified. These landmarks are currently used to prescribe standardized axial planes.

[0082] MRI scan planes and sequences are currently prescribed by technologists. Computer algorithms to automate each step of the clinical protocol have been developed and tested offline, as shown in Fig. 11. As an extension of this research, these algorithms will be fully integrated and optimized for real-time use on both clinical and investigational MRI scanners. Integration directly in the imaging pipeline will allow extensions of these algorithms to assess and compensate for patient motion between scans, ensuring optimally co-registered MR sequencing within and across studies, all prospectively registered in Talairach space (Weiss et al. 2002, 2003). By directly integrating MR scanners with algorithms that provide a reproducible and standardized anatomical space (Talairach space), an advanced platform for new anatomy-aware protocols will be created.

[0083] Because in some instances the algorithms may not be used in real-time, current use of the Talairach landmarks is limited to prescription of planes closely associated with the Talairach reference plane and manually selected by technologists, such as oblique axial MR parallel to the Talairach plane (Weiss et al. 2003). Integration into scanner software will enable the development of advanced protocols that include knowledge of brain anatomy as well as real-time adaptive "expert" scan protocols. Brain atlases will be used in real-time for prescription and these prescriptions will be entered in atlas coordinates. Expert systems will be developed and optimized using more complex anatomy-aware protocols involving iterative loops of real-time computer-aided detection of brain pathology to include stroke and aneurysms and brain protocols tailored specifically to the patient while within the magnet.

[0084] **Algorithms for scan prescription of MRI spine.** A fast rule-based spine contour extraction method has been developed. It consists of the following steps: 1) locating the inter-vertebral disc locations through angular projection of intensities over a small image window (Fig. 12a), 2) finding the inter-vertebral contour using a deformable contour

model (Fig..12b), and 3) locating the vertebral boundary and the spine contour (Fig. 12c). This method enables automated scan prescriptions, real-time lesion detection, and exam tailoring.

[0085] Recent advances in MRI to include the clinical implementation of phased array-coils and parallel sensitivity encoded imaging offer the potential for time and cost effective non-invasive holistic screening and detailed assessment of neuro-axis pathology, to include stroke and back pain--both leading causes of disability in the U.S. However, optimal patient evaluation requires individually optimized MRI sequencing, which in turn requires real-time analysis of increasingly complex and multi-parametric MR data. The development and integration of an automated system emulating/approximating detailed expert analysis while the patient is still in the magnet would significantly improve diagnostic imaging and medical care. Millions of MRI scans are performed each year, approximately 65% dedicated to the evaluation of the brain and spine. Software to synergistically improve the prescription and analysis of such scans has tremendous commercial potential. No such product is currently available and would be of great interest to both large medical imaging companies engaged in computer assisted medical imaging diagnosis.

[0086] **Medical Applications -- Detection and Analysis of Brain Pathology with MRI (Acute Stroke, Intracranial Aneurysms).** At UC Medical Center, Talairach referenced axial diffusion-weighted images (DWI), whether prescribed by a technologist or a computer, are currently obtained following the initial roll and yaw corrected sagittal T2 sequence. If computer image analysis of the initial DWI sequence suggests regions of acute infarction, the basic brain protocol would be streamlined and modified to include MR angiography and perfusion sequencing. This would respectively permit evaluation of the underlying vascular lesion and the detection of potential perfusion/diffusion mismatches directing emergent neuro-vascular intervention. Stroke is the leading cause of disability in this country. Because the time to emergent therapy strongly inversely correlates with morbidity and mortality, the development and implementation of the proposed computer algorithms could significantly improve patient outcome.

[0087] In conjunction with the Mayo Clinic, researchers at UC Medical Center are currently studying a large population of patients at risk for intra-cranial aneurysms using

MR angiography. One of the investigators (Dr. Weiss) has developed and implemented co-registered white and black blood MR angiography sequences which uniquely facilitates computer-aided diagnosis and analysis of potential aneurysms in this population. In the proposed work, such computer algorithms will be developed and their sensitivity will be compared against the expert standard (3 independent euroradiologists' assessments already in place). If computer image analysis of such initial MRA screening sequences reveals a potential aneurysm, dedicated phase-contrast images of the putative aneurysm could be iteratively prescribed to better characterize the lesion and assess flow characteristics.

[0088] Using computer flow modeling and other engineering analysis, the investigators plan to better stratify an individual aneurysm's risk for rupture, This could lead to more optimized patient management as the majority of brain aneurysms do not rupture and therapeutic intervention (coiling or clipping) carries morbidity and mortality risks. Tobacco smoking significantly increases the incidence ischemic brain disease as well as aneurysms and their rupture leading to catastrophic stroke.

[0089] **Detection and Analysis of Spine Pathology with MRI (Fractures, Disc Herniations).** Spine pathology is another leading cause of disability in this country. The proposed research will improve detection and assessment of disco-vertebral degeneration, osteoporotic and pathologic compression fractures-all potential underlying causes of ubiquitous back/neck pain in this country.

[0090] Using advanced MR imaging techniques, the entire spinal axis can be interrogated in the sagittal plane in less than a minute. With this screening data, the vertebral bodies and inter-vertebral discs can be identified and subsequently analyzed with the software proposed for development. Based on this initial assessment, regions of suspected pathology to include vertebral fractures and disc hernations, could be further interrogated with more dedicated computer driven prescriptions to confirm and better characterize pathology. If for example, a fracture is identified, additional multiparametric sequencing through the involved vertebrae would be obtained to determine whether the fracture was related to osteoporosis or underlying malignancy.

[0091] In conjunction, with the aforementioned software to iteratively prescribe and analyze brain MRI, the entire neuro-axis can be effectively screened and lesions

characterized in a single time-efficient scan session. Currently, such an examination is prohibitively lengthy and requires several imaging sessions if lesions were to be optimally characterized. Image analysis development for this MRI project should be synergistic with that done for the X-ray evaluation of vertebrae in the following section.

[0092] **Automated Subminute Submillimeter ResoIutionTotal Spine MRI Survey.**

[0093] **Purpose:** Develop and test an automated magnetic resonance imaging technique to rapidly survey the entire spine, enabling accurate unambiguous numbering and morphologic assessment of all intervertebral discs and vertebrae, as illustrated in FIGS. 13A-B.

[0094] **Materials & Methods:** Using commercial 1.5T MRJ systems equipped with 6-element spine array coils and 4-channel receivers, we tested overlapping and contiguous two-station sagittal fast gradient-echo sequencing with FOVs of 42 and 35cm respectively. Seven sagittal sections (4mm skip 1mm) were obtained at both superior and inferior spine stations (LI 5 - R15), matrix 512 x 352-420, 1 nex, flip angle 30 deg., utilizing minimum TRs to obtain 7 slices (58-62msec) and minimum TEs, the latter approximately 2.1 msec so that water and fat are out of phase at 1.5T. Ten de-identified two-station spine MRIs (5 with overlapping and 5 with contiguous sagittal acquisitions) were assessed by a neuroradiologist. The latter 5 studies were independently analyzed with a novel computer algorithm employing a disc projection matching and deformable contour model for automated identification, segmentation, and numbering of intervetebral discs and vertebrae. Vertebral body and disc-space numbering were compared . Results: Total scan time per station ranged from 21-23sec, providing an automated submillimeter in-plane resolution survey of the entire spine in less than 1 minute. In all cases, the neuroradiologist could unambiguously number all vertebrae and disc spaces from C2-3 through the sacrum, with discs demonstrating prominent hyperintensity and contrast against the vertebral bodies. Numbering from contiguous sagittal stations was more facile than from overlapping stations, taking the neuroradiologist only seconds. Computer-automated numbering for all 23 interspaces C2-3 through L5-S1 was concordant with the neuroradiologist's assignments in all five contiguous sagittal acquisition examinations reviewed. Additionally, the computer

program could generate disc and vertebral height measurements for all levels, though sampling completeness varied depending on patient positioning and scoliosis.

[0095] **Conclusion:** The entire spine can be surveyed with sub-millimeter in-plane resolution MRI in less than 1 minute with contiguous 35cm stations recommended. Given the ability to accurately number all vertebrae and discs visually or automatically with computer software, we have clinically instituted and recommend this protocol as an integral part of the localizer set-up for all thoracic and/or lumbar MRI studies. With additional software development and scanner integration, this technique may provide computer- automated iterative spine prescriptions as previously suggested for brain MRI. (Weiss 2003) Reference: Weiss KL, Pan H, Storrs J. Strub W, Weiss JL, Eldevik OP. Clinical Brain MRI Prescription in Talairach Space: Technologist and Computer Driven Methods. AJNR;May 2003:922-929.

[0096] Automated Spine MRI for Rapid Osteoporosis Screening. Novel MRI technique provides efficient screening and iterative assessment of patients at risk for osteoporotic spine fractures.

[0097] Aims: (1) Refine our novel Automated Spine Survey Iterative Scan Technique (ASSIST) to optimize sub-minute morphologic screening of entire spine with MRI; (2) Combine technique with investigational 3-point Dixon methodology to provide quantitative assessment of vertebral marrow fat fraction (F%) and cancellous bone-induced intravoxel spin dephasing rate (R2*); and (3) Perform multi-variate analysis to model vertebral fracture risk as approximated by #1, with F%, R2*, and spinal dual-energy x-ray absorptiometric (DEXA) bone mineral density (BMD).

[0098] Osteoporosis is a disease characterized by low bone mineral density and abnormal bone microarchitecture. Currently, it affects about 30% of post-menopausal women, with more than 50% at risk. With our population rapidly aging, the prevalence of osteoporosis continues to rise. As osteoporotic-related fractures result in major morbidity, health care expenditures, and mortality in the elderly, this proposal addresses the DDF's desire to promote research in Aging-Geriatrics. Moreover, by applying cutting-edge investigational technology to this critical health-care problem, the study fulfills Translational Research Initiative goals as well.

[0099] The traditional criterion for assessing fracture risk is bone mineral density (BMD) as may be measured by single-photon absorptiometry (SPA), quantitative computed tomography (QCT), single-energy x-ray absorptiometry (SXA), and most commonly dual-energy x-ray absorptiometry (DEXA). Unfortunately, while negatively correlated with fracture risk, BMD by itself remains an unsatisfactory predictor. Consequently, investigational work has increasingly focused on ultrasound and MRI. The latter technique has the unique potential to quantify fractures, which are highly correlated with subsequent risk of fracture; differentiate between osteoporosis and other underlying pathology, such as metastases; and target therapy such as vertebroplasty. MRI researchers have also demonstrated improved fracture risk prediction by combining DEXA measurements with Dixon sequence derived F% (positively correlated) and R2* (negatively correlated). Unfortunately, MRI of the spine has been too time intensive and costly to justify as an osteoporosis-screening instrument.

[00100] To rectify this important shortcoming, we propose integration of the 3-point Dixon technique with our novel automated sub-minute sub-millimeter resolution total spine screen. This should afford rapid high-resolution morphometric assessment, as well as, the separation and quantification of fat, water, and R2*. We plan to test this methodology on 50 post-menopausal women who have been referred for a DEXA scan.

[00101] While the present invention has been illustrated by description of several embodiments and while the illustrative embodiments have been described in considerable detail, it is not the intention of the applicant to restrict or in any way limit the scope of the appended claims to such detail. Additional advantages and modifications may readily appear to those skilled in the art.

[00102] What is claimed is:

Claims

1. A method for performing a medical diagnostic imaging scan of a patient, comprising:

placing a longitudinally unique opaque spinal coil on external to a spine of a patient;

performing a scout scan;

identifying and labeling on diagnostic scans each vertebral body of the spin;

autoprescribing a portion proximate to a vertebral body for a detailed scan;

identifying a unique longitudinal position of the spinal coil proximate to a surgical site contained within the autoprescribed portion; and

inserting a therapeutic instrument localized by the spinal coil to the surgical site.

INTEGRATED MULTIMODALITY MULTIFUNCTIONAL SPATIAL REFERENCE AND SKIN/SURFACE MARKING SYSTEM AND AUTOMATED SPINE MRI / CT RAPID AUTOPRESCRIPTION

Abstract of the Invention

An integrated self adhesive spatial reference and skin marking system is designed for a variety of modalities to include MRI, CT, SPECT, PET, planar nuclear imaging, radiography, XRT, thermography, optical imaging and 3D space tracking. The device ranges from a point localizer to a more multifunctional and complex grid/phantom system. The specially designed spatial reference(s) is affixed to an adhesive strip with corresponding markings so that after applying the unit to the skin/surface and imaging, the reference can be removed leaving the skin appropriately marked. The localizer itself can also directly adhere to the skin after being detached from the underlying strip.

BEST AVAILABLE IMAGES

Defective images within this document are accurate representations of the original documents submitted by the applicant.

Defects in the images may include (but are not limited to):

- BLACK BORDERS
- TEXT CUT OFF AT TOP, BOTTOM OR SIDES
- FADED TEXT
- ILLEGIBLE TEXT
- SKEWED/SLANTED IMAGES
- COLORED PHOTOS
- BLACK OR VERY BLACK AND WHITE DARK PHOTOS
- GRAY SCALE DOCUMENTS

IMAGES ARE BEST AVAILABLE COPY.

As rescanning documents *will not* correct images, please do not report the images to the Image Problem Mailbox.

Fig 1

Fig 1 cont.

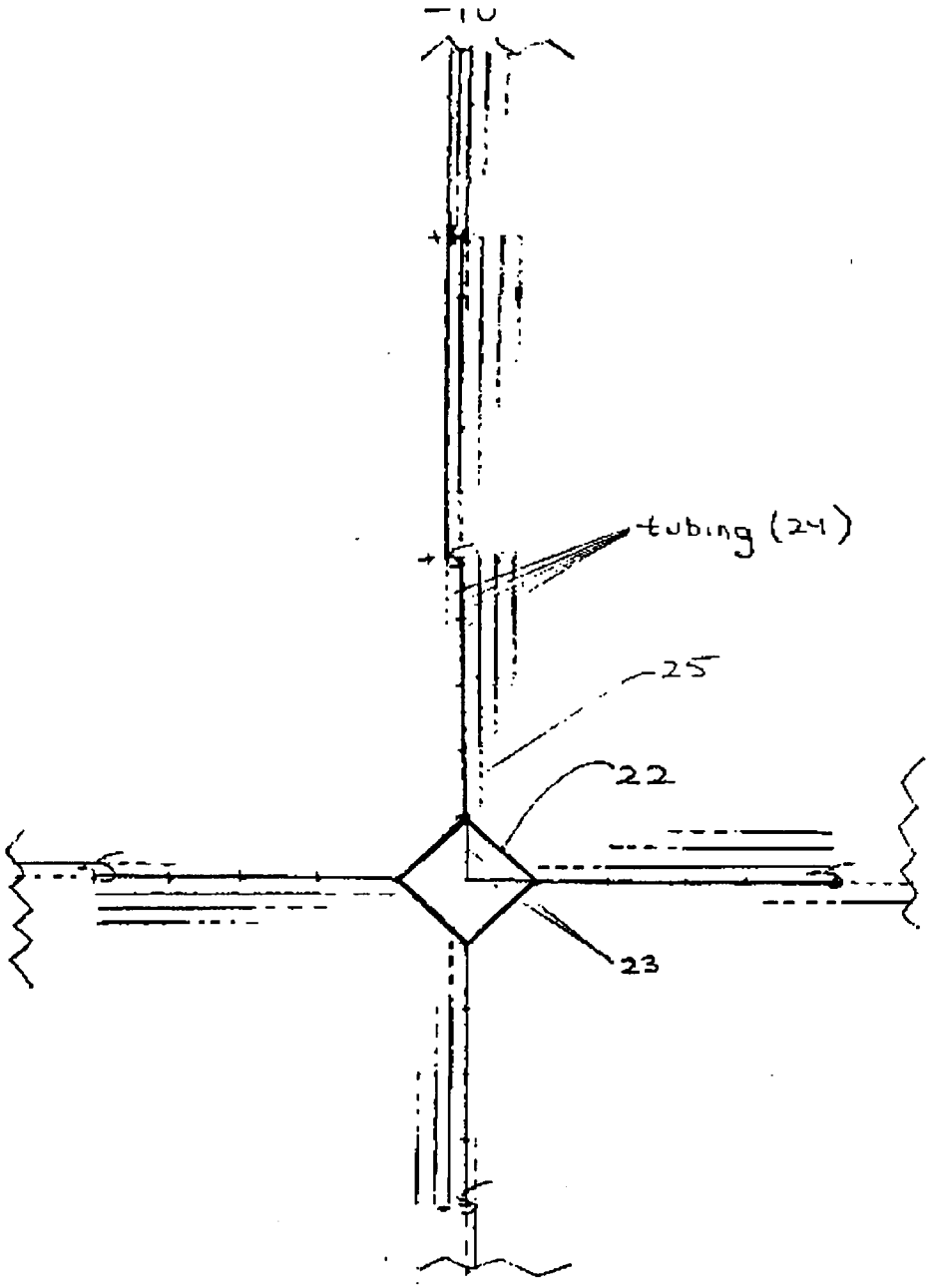

Fig 2a

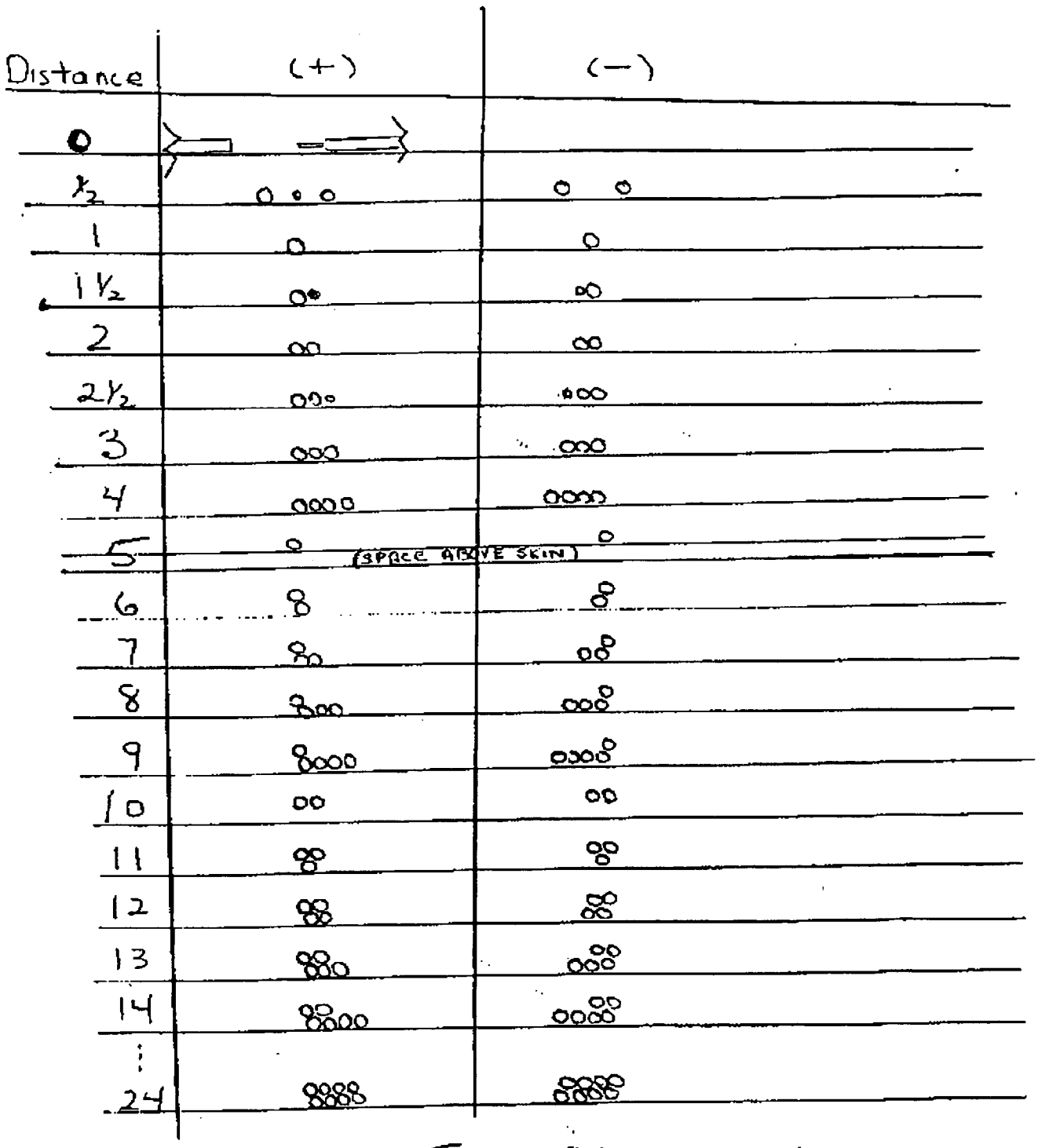

Fig 2b

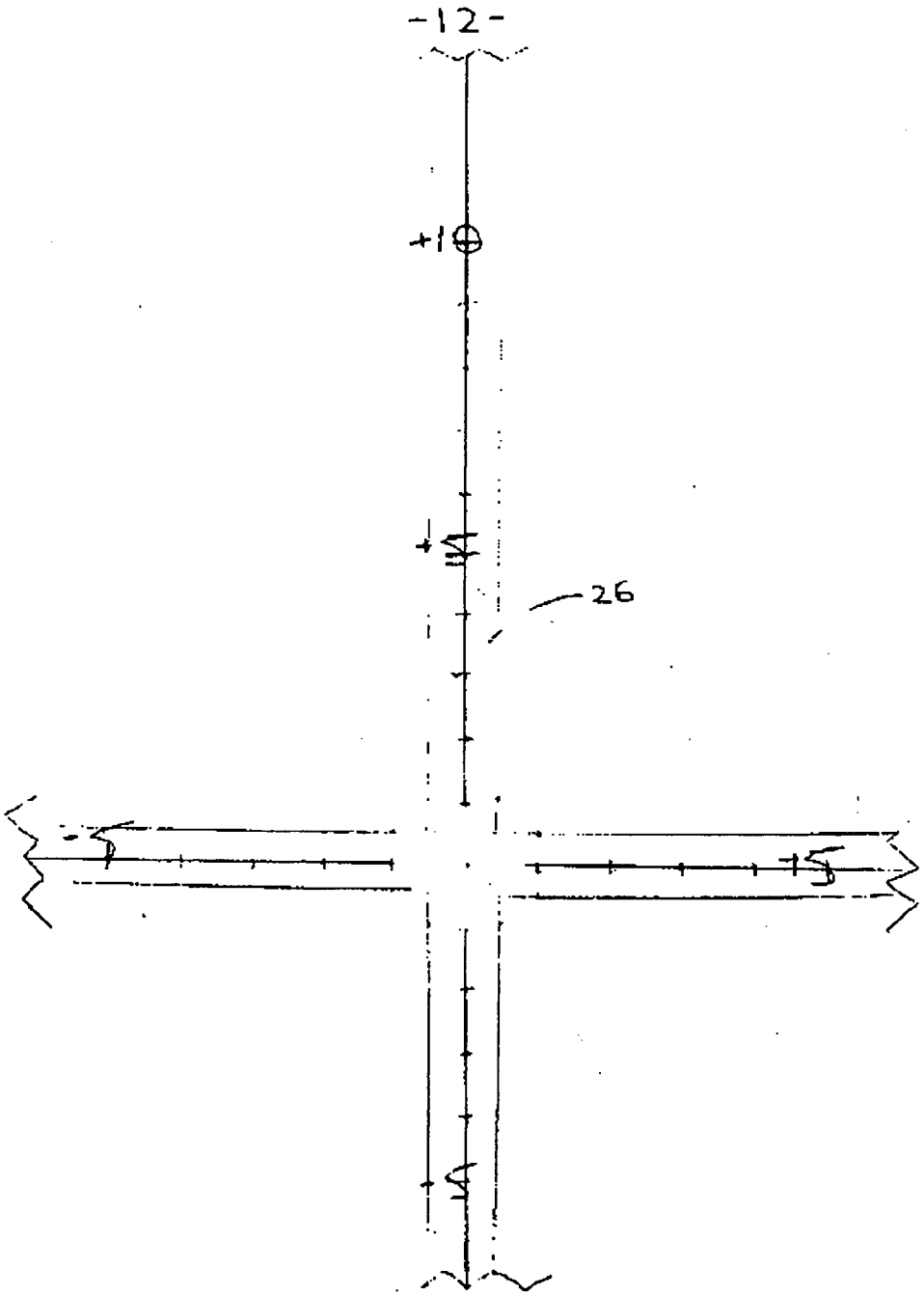

Fig 2c

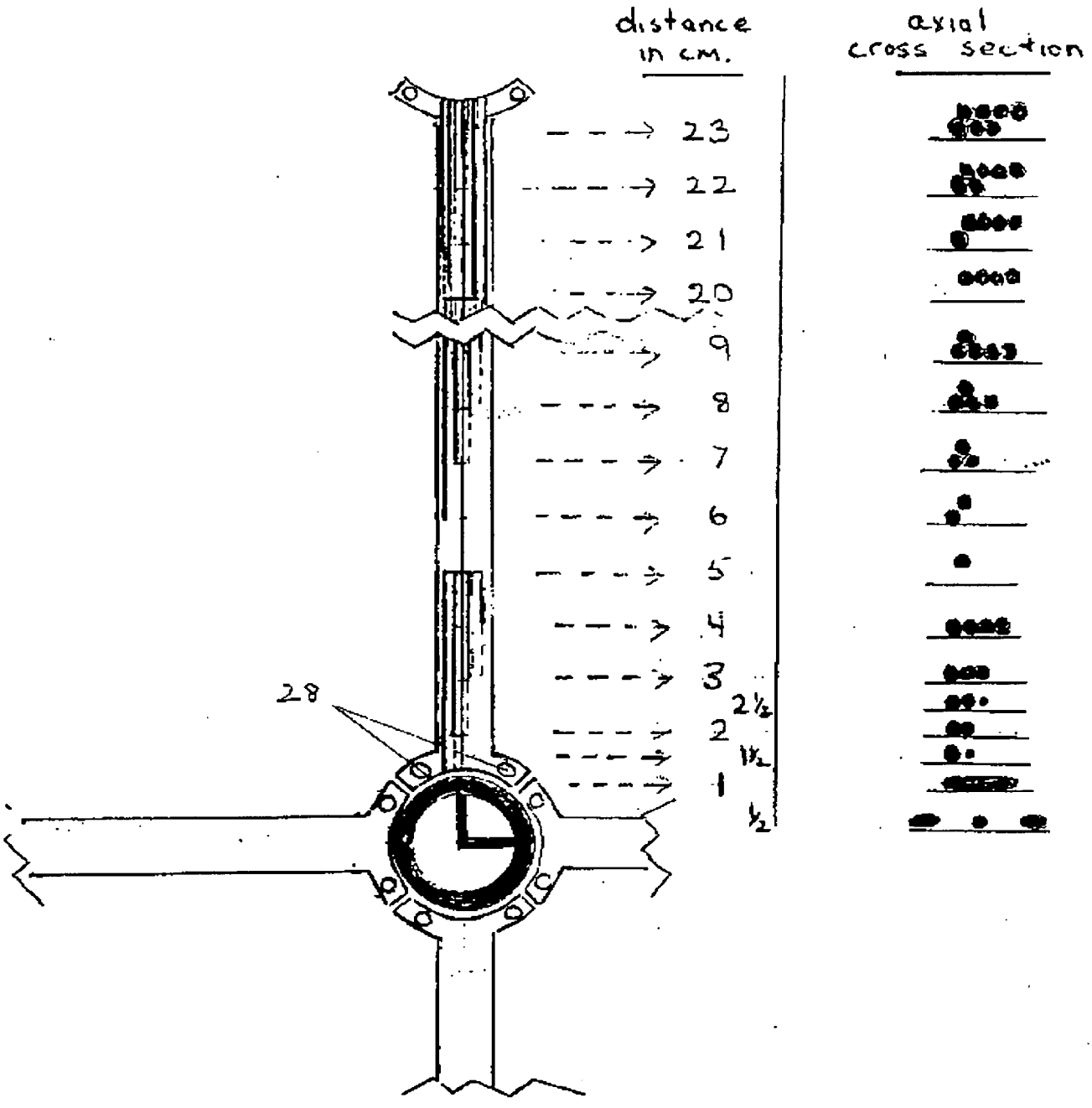
distance in cm.
axial cross section
23
22
21
20
9
8
7
6
5
4
3
2
1
2½
1½
½
28

Fig 2d

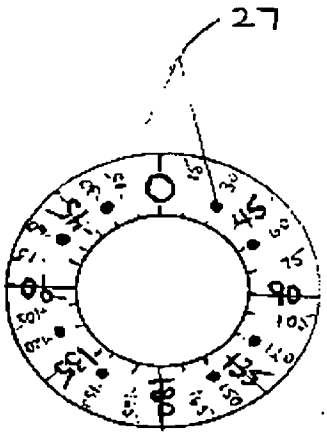

Fig 2e

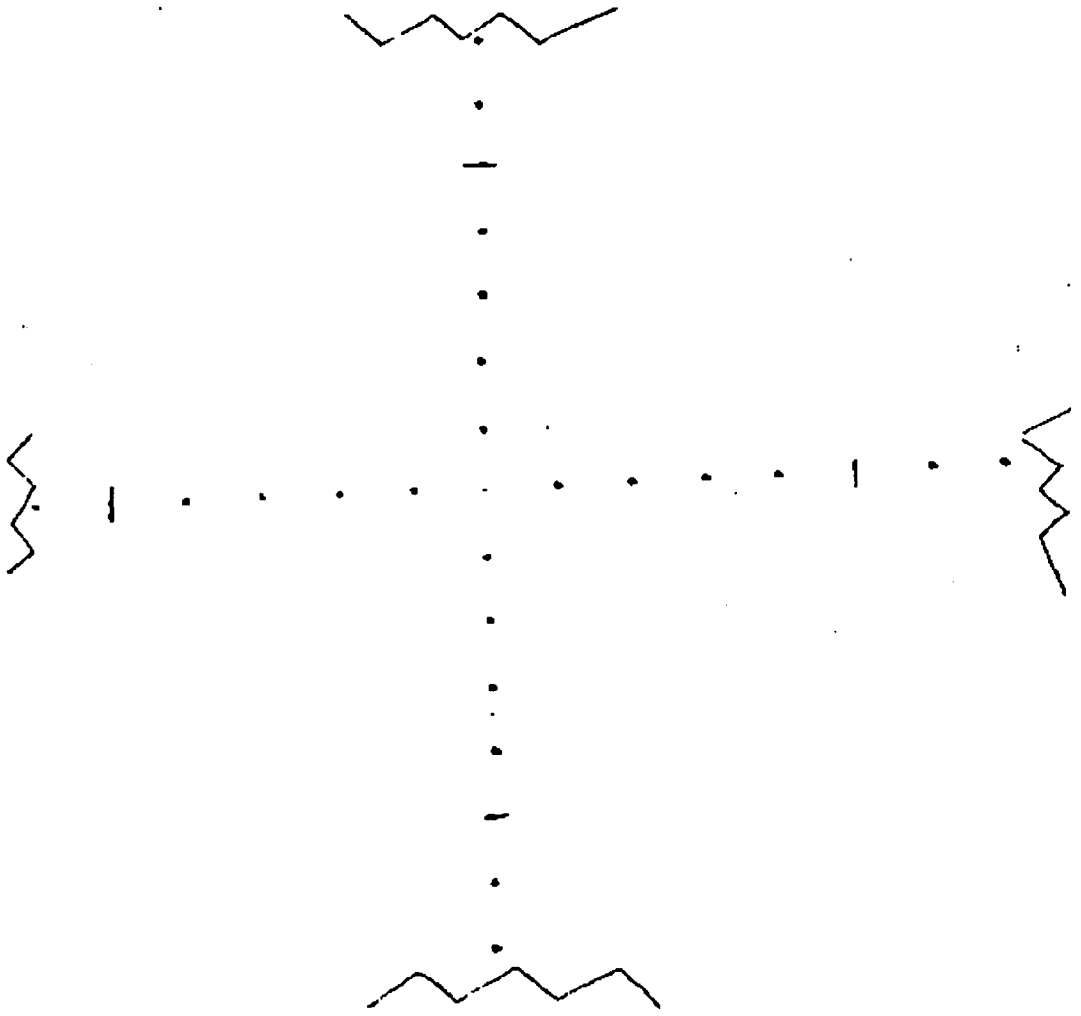

Fig 2f

Fig 3

Addendum

Two additional variations are now described, potentially replacing the somewhat complex cross design (fig 2) with an extension of the basic point localizer (Fig 1) or modification of the planar phantom/localizer (Fig 3). These changes may further simplify and unify the proposed marking system.

In the first instance, rather than packaging the ring localizers in a sheet as illustrated in Fig 1i , they could be packaged in a strip or roll, regularly spaced at 5 cm or other intervals (Fig 4a). The strip with attached ring and /or cross localizers could then serve as a linear reference of any desired length. By placing two strips orthogonally, a cross shaped grid is created. Individual rings can be removed from the strip or rotated to customize the grid as desired (Fig 4b).

In the second instance, by slightly modifying the square design illustrated in Fig 3, an elongated rectilinear or cross configuration (Fig 4a) is achieved consisting of linearly arranged squares extending vertically and/or horizontally from the central square. One tube in each of these squares will have a larger diameter than the other similarly oriented tubes as determined by the square's distance from the isocenter. For example, the square centered 10cm above the isocenter would have its first tube situated to the right of midline given an increased diameter and the square centered 20 cm above the isocenter would have its second tube to the right of midline given an increased diameter and so on.

Cross sectional distance from isocenter would be read by adding the distance determined by each square's diagonally oriented slice indicator to 10 times the numberline position of the largest diameter tube. Figure 5b illustrates the cross sectional appearance of an axial section obtained 12 1/2 cm. above isocenter. By adding 2 1/2 (the slice indicator position) to 10 times 1 (the tube with largest diameter), distance is readily determined.

Alternatively, the caliber of all tubes could be kept constant and instead an additional diagonal indicator tube passing through isocenter added for each elongated axis (vertical with slope of 10 and horizontal with slope of 1/10). Cross sectional distance from isocenter would then be determined by looking at the position of both the additional and original diagonal indicator tubes in reference to the cross sectionally created number line.

It should also be noted that localizer grids similar to those illustrated in Figs 3 and 5 could be constructed of barium (or other high x-ray attenuative material) impregnated sheets rather than tubes if computed tomography is the primary imaging modality desired and phantom attenuation values are not needed. This would significantly reduce the cost of the grid, allowing disposability and retaining 1:1 compatibility with the multifunctional tube filled grid/phantom.

Fig 4

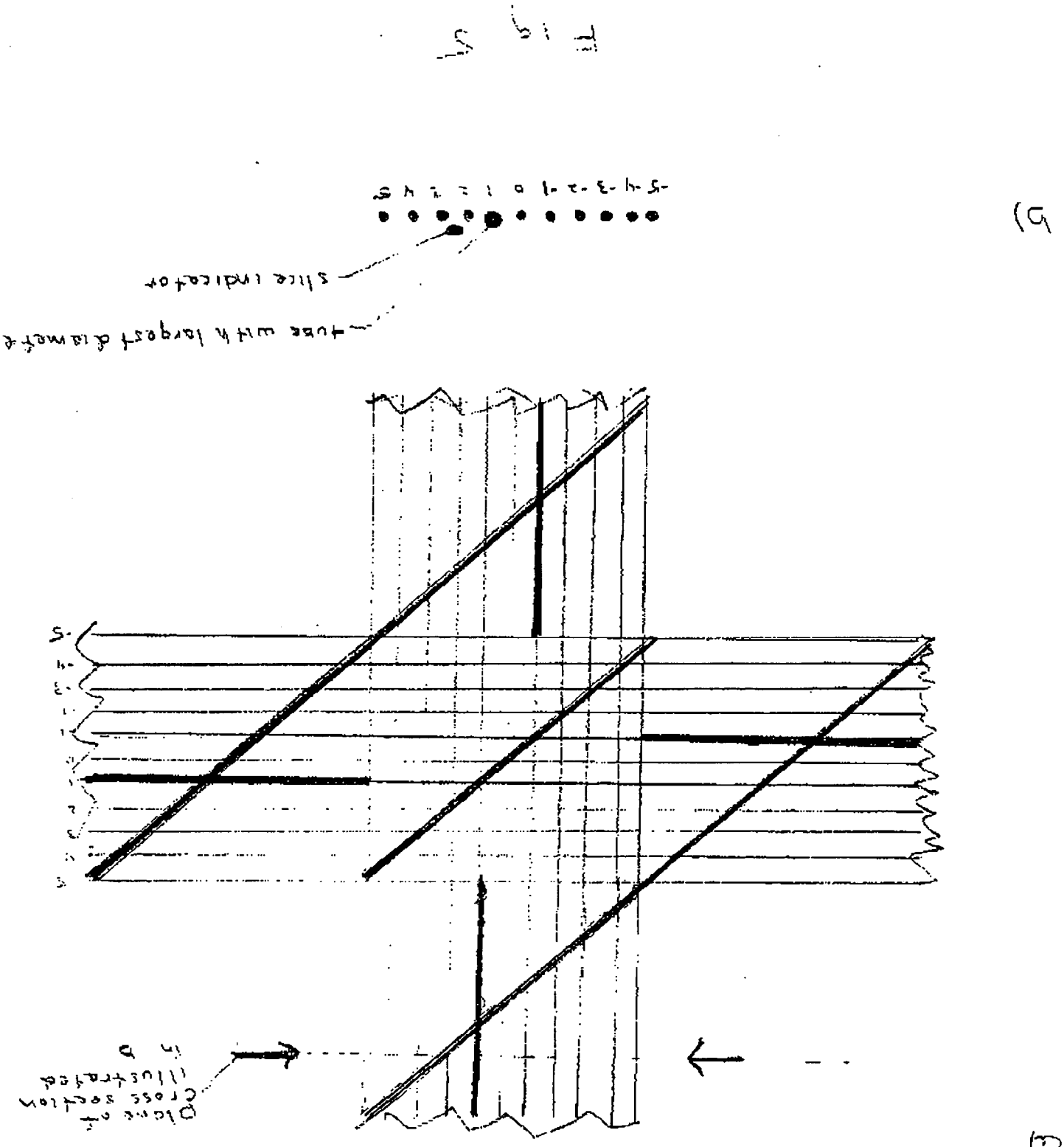

~ 1/4 scale

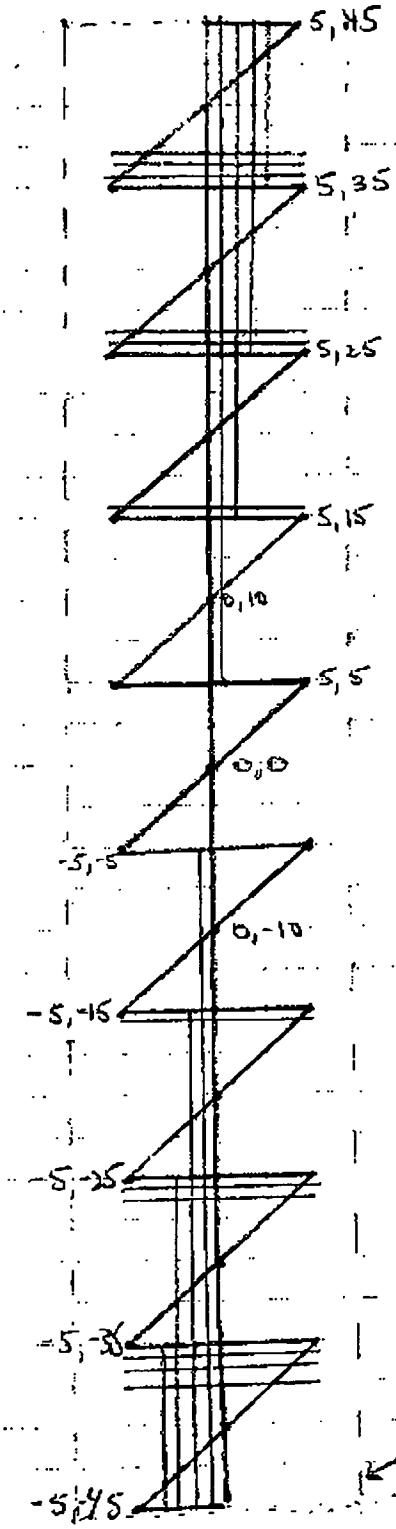

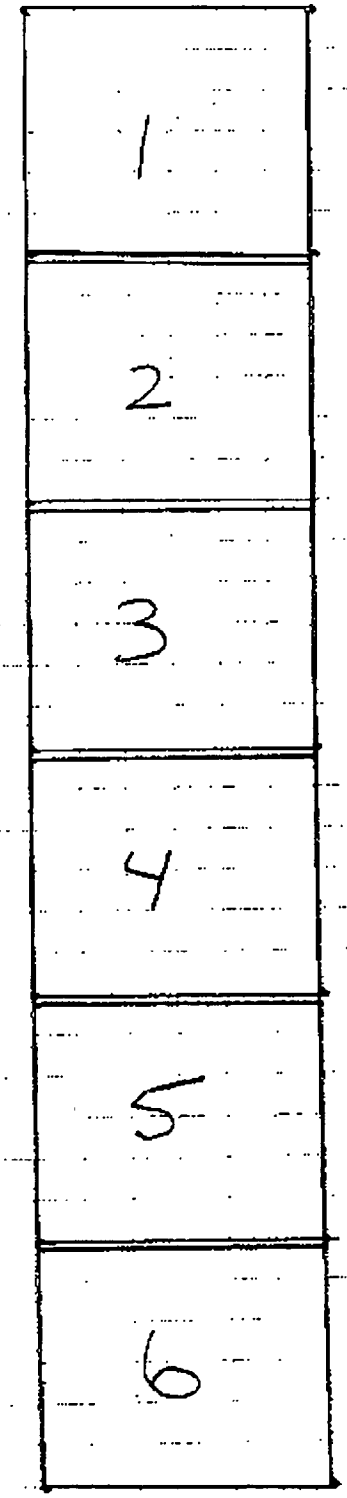

← Sheath for

Fig 6a) 90×10 cm grid localizer

6b) 6-element array coil

1:1 scale

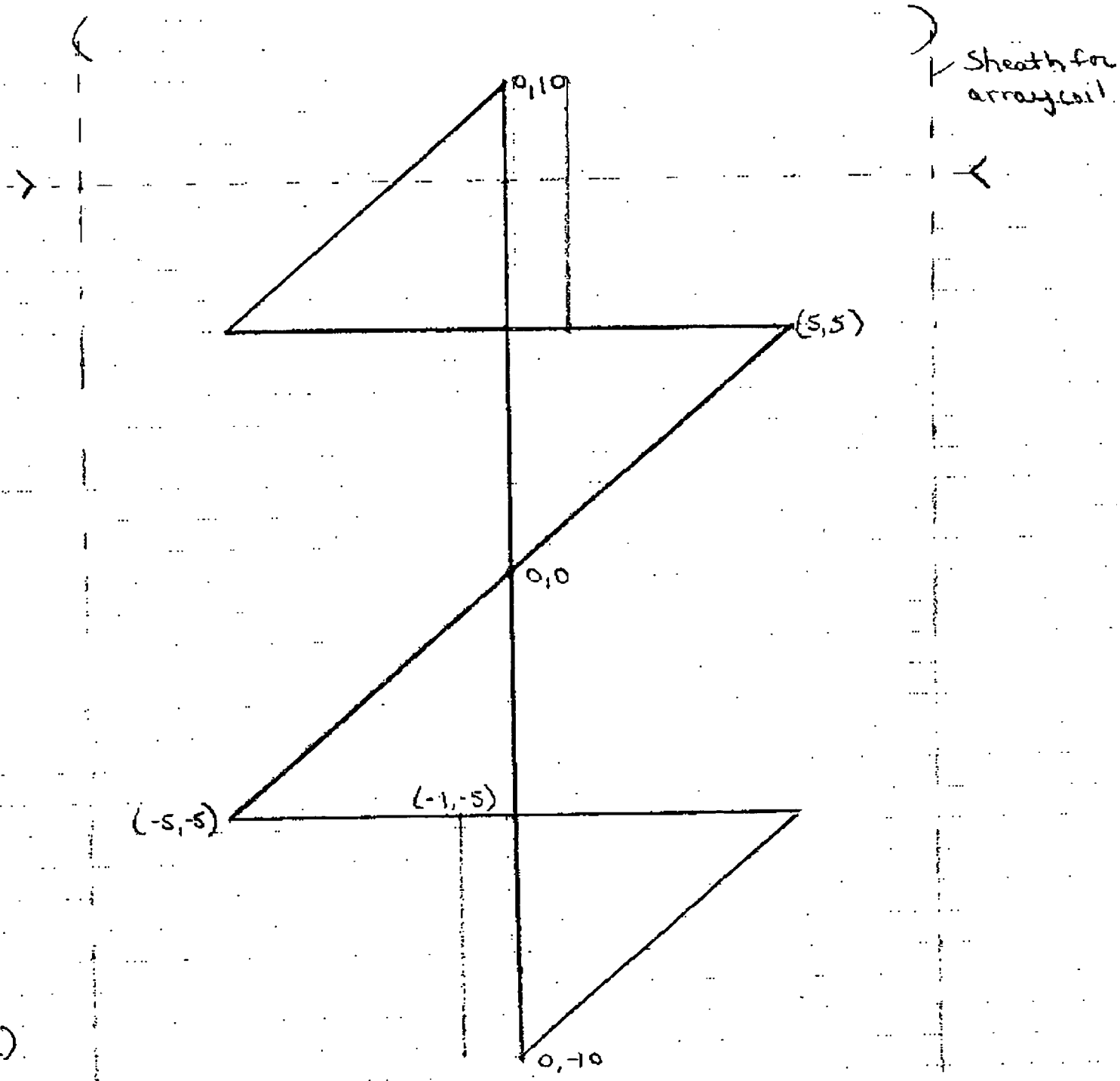

6c)

6d) $y = 8$

AXIAL CROSS SECTION

= 2 cm

1 cm (x10)

$y = (1 \times 10) - 2 = 8$ cm

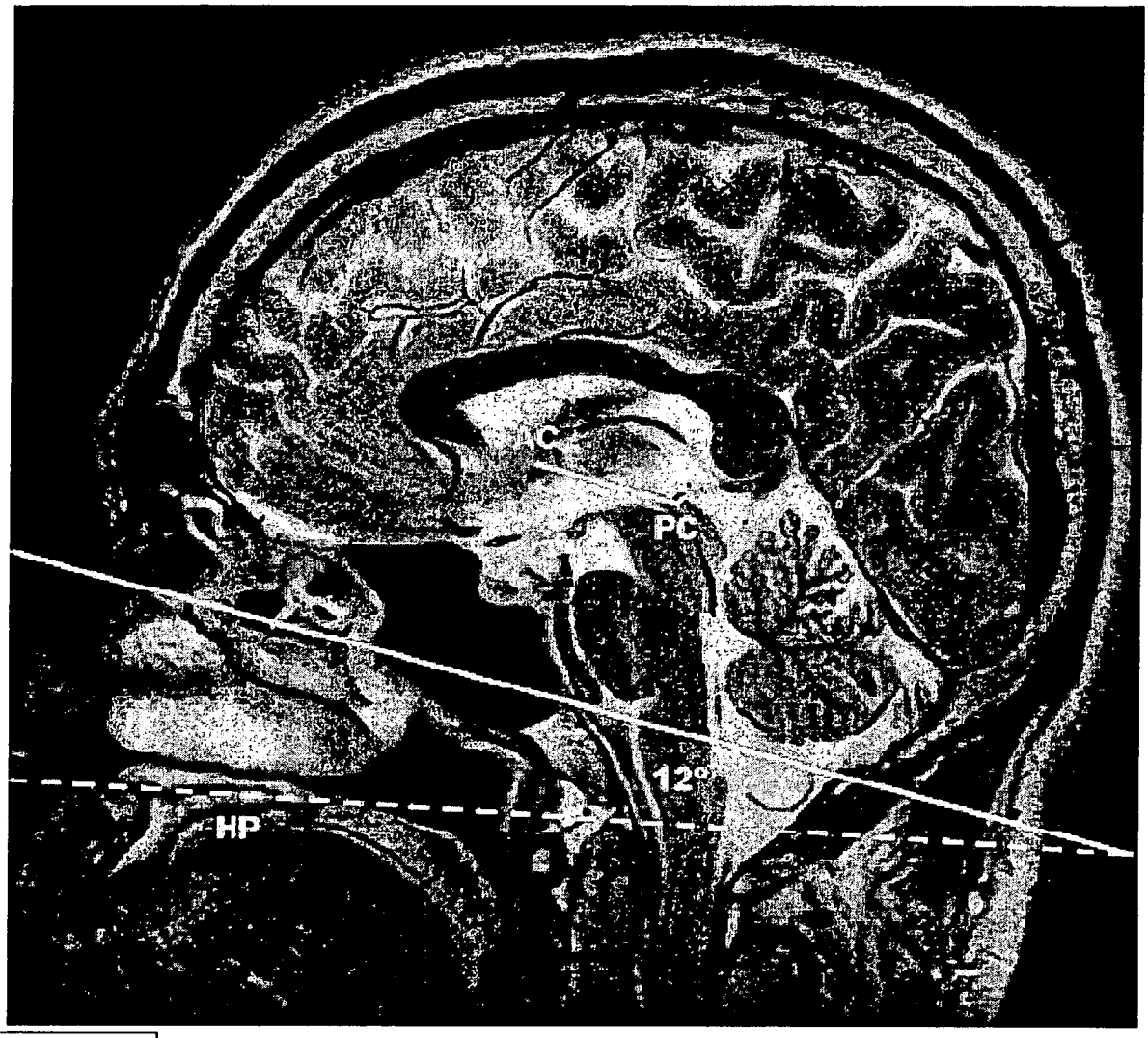

FIG. 7 Midline roll- and yaw-corrected sagittal fast spin-echo T2-weighted MR image (TR/TE, 3816/105$_{eff}$;echo train length, 16; section thickness, 4 mm; matrix 512 × 256; field of view, 20 cm). The short solid line corresponds to the Talairach AC-PC basal reference; The long solid line is drawn parallel to the Talairach AC-PC reference, and the dashed line passes through the superior cortical surface of the hard palate. Note in this prototypical case the angle subtended by the Talairach AC-PC line and the hard palate is 12°. AC, anterior commissure; PC, posterior commissure; HP, hard palate.

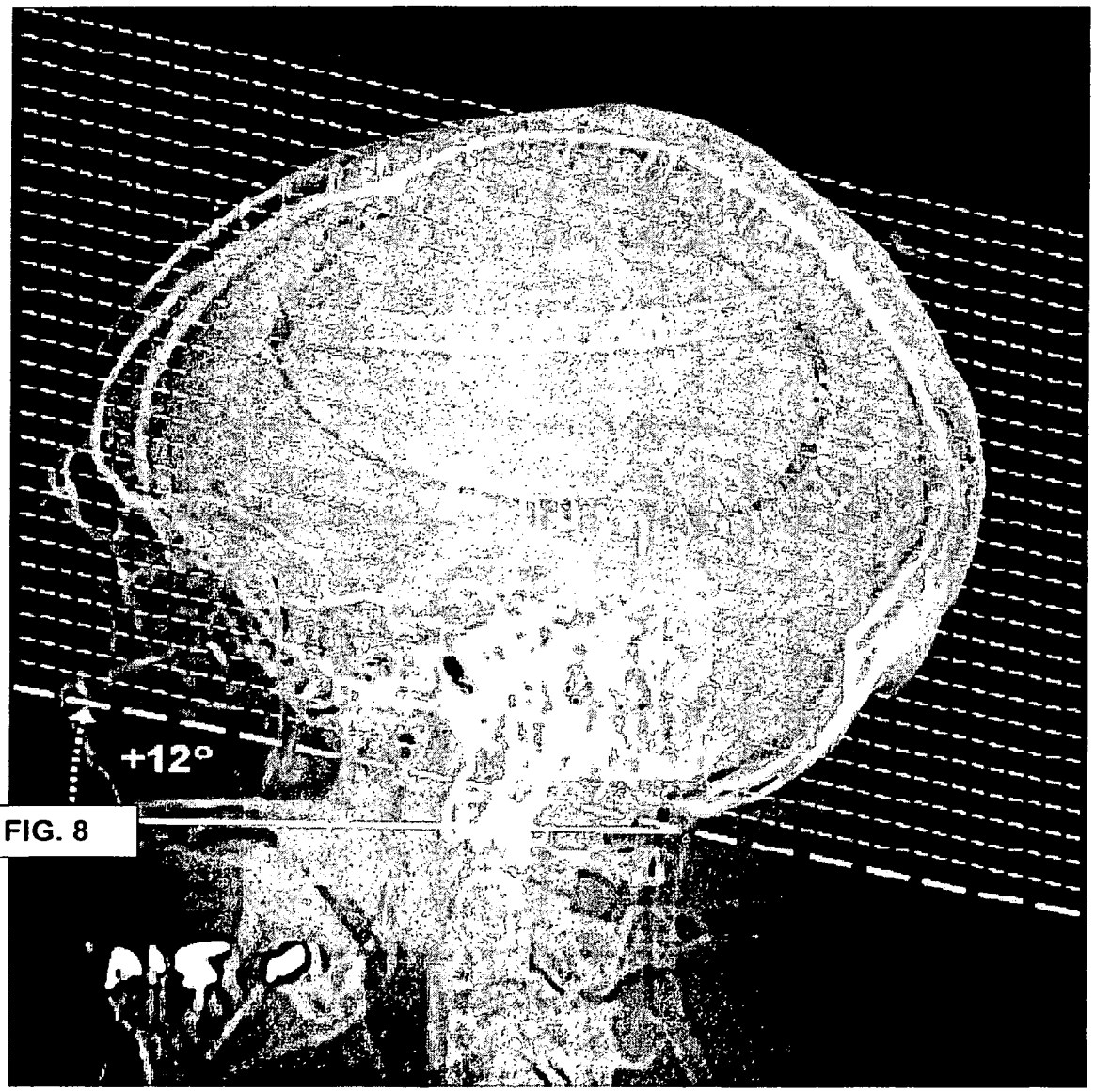

FIG. 8

FIG 2. Lateral CT scout view from a study patient illustrating the axial scan prescription (*dotted lines*) with the HP+12 protocol angled +12° from a line passing through the hard palate (*solid line*). The solid line indicating the orientation of the hard palate has been offset a few millimeters inferiorly to provide a clear view of the hard palate.

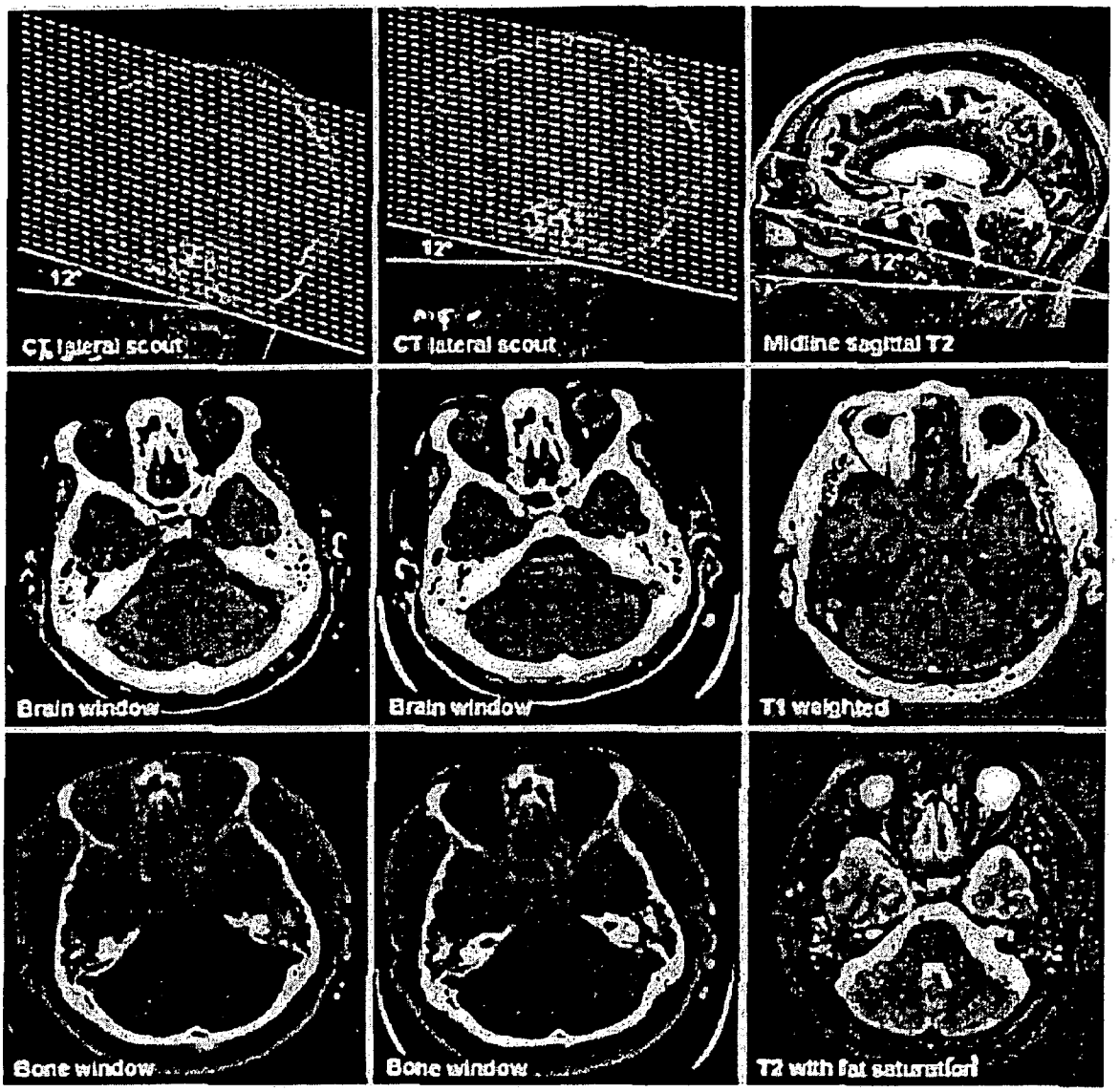
12°
CT lateral scout
12°
CT lateral scout
Midline sagittal T2
Brain window
Brain window
T1 weighted
Bone window
Bone window
T2 with fat saturation

FIG. 9

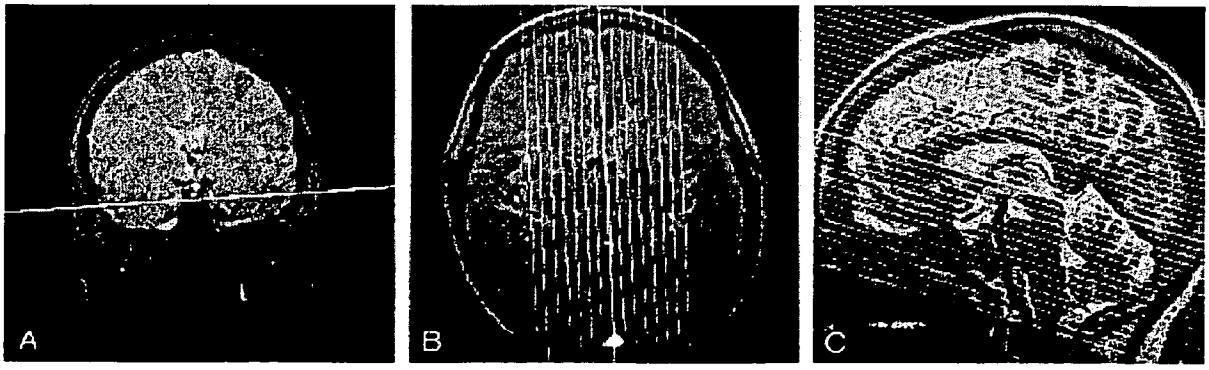
A
B
C

FIG. 10

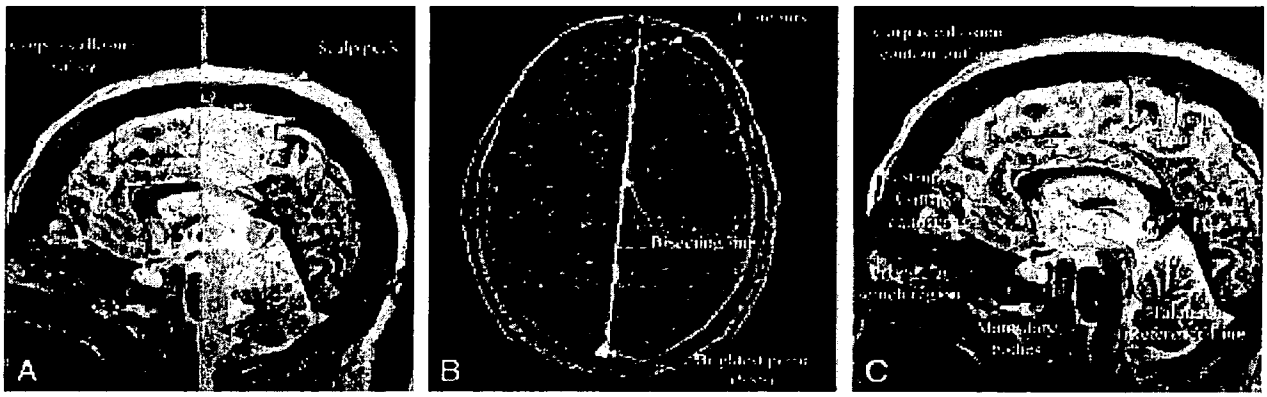

FIG. 11

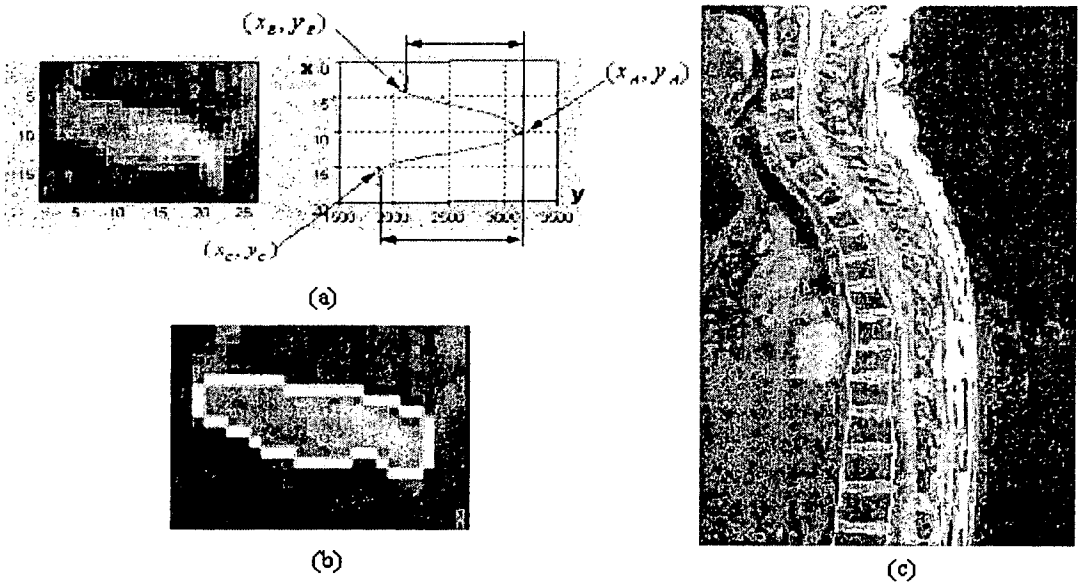

FIG. 12

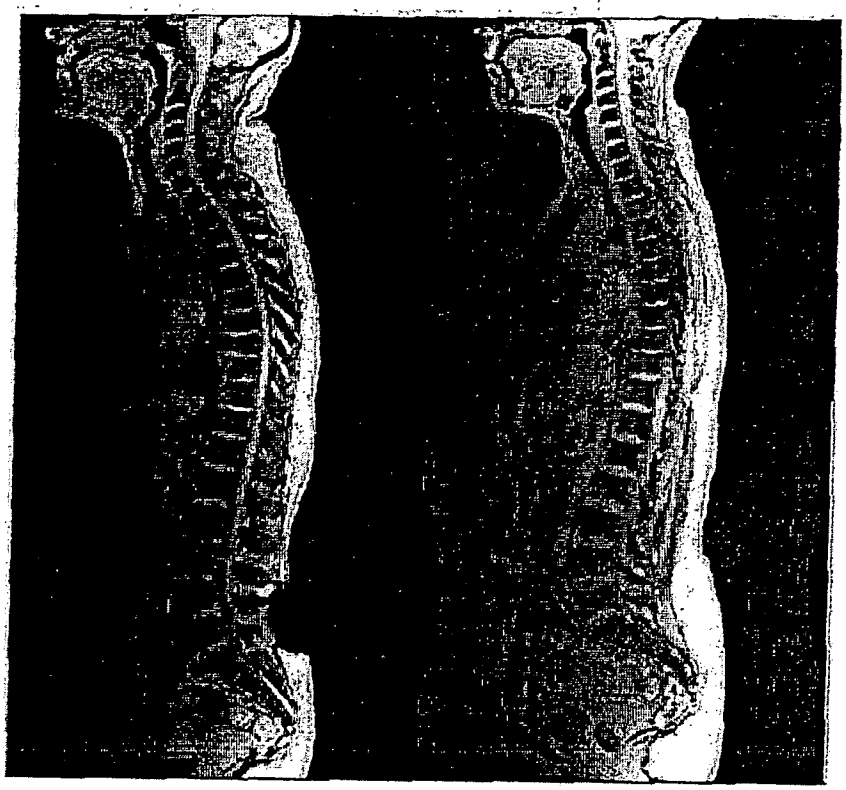

FIGS. 13A-B